Manuscript prepared for Biogeosciences
with version 2014/09/16 7.15 Copernicus papers of the LaTeX class copernicus.cls.
Date: 24 August 2015

Air-sea CO_2 fluxes and the controls on ocean surface pCO_2 seasonal variability in the coastal and open-ocean southwestern Atlantic Ocean: A modeling study

Ricardo Arruda[1], Paulo H. R. Calil[1], Alejandro A. Bianchi[2,3], Scott C. Doney[4], Nicolas Gruber[5], Ivan Lima[4], and Giuliana Turi[5,6]

[1]Laboratório de Dinâmica e Modelagem Oceânica (DinaMO), Instituto de Oceanografia, Universidade Federal do Rio Grande, Rio Grande, RS, Brazil.
[2]Departamento de Ciencias de la Atmósfera y los Oceános, Universidad de Buenos Aires, Buenos Aires, Argentina.
[3]Departamento Oceanografía, Servicio de Hidrografía Naval, Av. Montes de OCA2124- Buenos Aires, Argentina
[4]Department of Marine Chemistry and Geochemistry, Woods Hole Oceanographic Institution, Woods Hole, MA, USA.
[5]Institute of Biogeochemistry and Pollutant Dynamics, ETH Zurich, Zurich, Switzerland.
[6]Now at: CIRES, University of Colorado at Boulder, and NOAA/ESRL, Boulder, CO, USA.

Correspondence to: Ricardo Arruda (cadoarruda@gmail.com)

Abstract. We use an eddy-resolving, regional ocean biogeochemical model to investigate the main variables and processes responsible for the climatological spatio-temporal variability of pCO_2 and the air-sea CO_2 fluxes in the southwestern Atlantic Ocean. Overall, the region acts as a sink of atmospheric CO_2 south of ~~30° S~~30°S, and is close to equilibrium with the atmospheric CO_2 to the north. On the shelves, the ocean acts as a weak source of CO_2, except for the mid/outer shelves of Patagonia, which act as sinks. In contrast, the inner shelves and the low latitude open ocean of the southwestern Atlantic represent source regions. Observed nearshore-to-offshore and meridional pCO_2 gradients are well represented by our simulation. A sensitivity analysis shows the importance of the counteracting effects of temperature and dissolved inorganic carbon (DIC) in controlling the seasonal variability of pCO_2. Biological production and solubility are the main processes regulating pCO_2, with biological production being particularly important on the ~~shelf regions~~shelves. The role of mixing/stratification in modulating DIC, and therefore surface pCO_2, is shown in a vertical profile at the location of the Ocean Observatories Initiative (OOI) site in the Argentine Basin (~~42° S, 42° W~~42°S, 42°W).

1 Introduction

Shelf regions are amongst the most biogeochemically dynamical zones of the marine biosphere (Walsh, 1991; Bauer et al., 2013). Even though they comprise only $7-10\%$ of the global ocean

area (Laruelle et al., 2013), continental shelves could contribute to approximately $10-15\%$ of the ocean primary production and 40% of the ocean's carbon sequestration through particulate organic carbon (Muller-Karger et al., 2005). Global discussions about the role of continental margins as a sink of atmospheric CO_2 gained momentum after Tsunogai et al. (1999) ~~, who~~ suggested that these shelf regions take up as much as 1 PgC/year of atmospheric CO_2. Recent estimates range from 0.2 PgC/year (Laruelle et al., 2013) to ~~0.589~~ roughly 0.6 PgC/year (Yool and Fasham, 2001), somewhat more modest than initially thought (Gruber, 2015), but still relevant to the global ocean sink estimated around 2.3 PgC/year (Ciais et al., 2014).

Continental shelves tend to act as a sink of carbon at high and medium latitudes ($30^\circ - 90^\circ$), and as a weak source at low latitudes ($0^\circ - 30^\circ$) (Chen et al., 2013; Hofmann et al., 2011; Bauer et al., 2013; Laruelle et al., 2014), i.e., they tend to follow similar meridional trends as the open ocean CO_2 fluxes (Landschützer et al., 2014; Takahashi et al., 2009).

However, continental shelves present a higher spatio-temporal variability of air-sea CO_2 fluxes than the adjacent open ocean, with the inner shelf and near coastal regions generally acting as a source of CO_2 to the atmosphere, while the mid/outer shelf and the continental slope generally ~~acting as sink~~ act as sinks (Cai, 2003). This pattern can be explained by the increased primary production and decreased terrestrial supply towards the outer shelf (Walsh, 1991). Seasonality of the upper ocean (e.g. mixing and stratification) may also be important to the air-sea exchange of carbon. For example, the United States southeast continental shelf acts as a sink of CO_2 in the winter and as a source in the summer (Wang et al., 2005).

In the southwestern Atlantic Ocean, the shelf region presents distinct features. To the south, the Patagonian shelf is one of the world's largest shelves with an area close to 10^6 ~~km^2~~ km^2, broadening to more than 800 km from the coastline (Bianchi et al., 2009). To the north, the Brazilian shelf narrows to around 100-200 km from the coastline. This region is ~~characterized as~~ one of the most energetic regions of the world's ocean with the confluence of the warm southward-flowing Brazil Current (BC) and the cold Malvinas Current (MC) flowing northward (Piola and Matano, 2001). The extension of the confluence roughly divides the subtropical and subantarctic oceanic gyres in the South Atlantic and ~~maybe~~ might be a hotspot for shelf-open ocean exchange (Guerrero et al., 2014).

~~This area~~ In the open-ocean, the South Atlantic is thought to absorb between 0.3-0.6 PgC/year south of ~~30° S~~ 30°S, while acting as a source to the atmosphere north of ~~30° S~~ 30°S (Takahashi et al., 2002). Aside from global open-ocean estimates, only a few local studies were conducted on the continental shelves in this region. The ~~Patagonian~~ Patagonia shelf was characterized as a source of CO_2

to the atmosphere on the inner shelf, and as a sink in the mid-outer shelf (Bianchi et al., 2009). The southeast Brazilian shelf and continental slope were characterized as sources of CO_2 to the atmosphere during all seasons (Ito et al., 2005). Such regions are often neglected, or poorly resolved, on relatively coarse global modelling assessments, although they may contribute up to 0.2 PgC/year of global ocean CO_2 uptake (Laruelle et al., 2014).

Regional marine biogeochemical models have been used to assess the ocean carbonate system and CO_2 fluxes, including the continental margins. For example, along the US east coast, the seasonality of pCO_2 was found to be controlled mainly by changes in the solubility of CO_2 and biological processes (Fennel and Wilkin, 2009). Along the California coast, biological production, solubility and physical transport (e.g. circulation) were found to be the most influential processes on pCO_2 variability, both ~~spatial and temporal~~ spatially and temporally (Turi et al., 2014).

In this study we use a regional marine biogeochemical model coupled to a hydrodynamic model to investigate the parameters and processes regulating the variability of ocean surface pCO_2 in the southwestern Atlantic Ocean. Our model domain includes the ~~region of the~~ location of the global node mooring that is soon to be deployed as part of the Ocean Observatories Initiative (OOI) ~~Argentine global node~~ at 42°S, 42°W (oceanobservatories.org).

We compare modeled surface pCO_2 distribution with observations and use the results to investigate the relative importance of the parameters (DIC, temperature, alkalinity and salinity) and processes (biological production, air-sea CO_2 flux, CO_2 solubility and physical transport) in controlling surface pCO_2 distribution and variability on the continental shelf and open ocean in the ~~Southwest~~ southwestern Atlantic Ocean.

2 Materials and Methods

2.1 Model

The physical model used in this study is the Regional Ocean Modeling System (ROMS) (Shchepetkin and McWilliams, 2005). Our model domain ~~in~~ spans from 15°S to 55°S, and from 70°W to 35°W, i.e., covering the southwestern Atlantic ~~Ocean spans from~~ from its subtropical to subantarctic ~~oceanic regions (15^oS to 55^oS)~~ latitudes and from the continental ~~shelves~~ shelf all the way out to the open ocean~~($70°W$ to $35°W$)~~. The horizontal grid resolution is 9 km, with 30 vertical levels with increasing resolution towards the surface.

The biogeochemical model is an NPZD type, including the following state variables: phytoplankton, zooplankton, nitrate, ammonium, small and large detritus, and a dynamic chlorophyll to carbon ratio for the phytoplankton (Gruber et al., 2006). A carbon component is also coupled to the model, with the addition of calcium carbonate, DIC and alkalinity to the system of state variables (Gruber et al., 2011; Hauri et al., 2013; Turi et al., 2014). Parameters utilised in the biogeochemical model are listed in Table ~~??~~1 of Gruber et al. (2006), and the $CaCO_3$ parameters as in Hauri et al. (2013). These parameters represent phytoplankton types ~~,~~with large nutrient requirements and relatively fast growth rates, usually large organisms (Gruber et al., 2006). Since our domain encompasses several ecological provinces (Gonzalez-Silvera et al., 2004), we may not represent all regions equally well with only one phytoplankton functional type.

The initial and boundary conditions used for the physical variables were obtained from a climatology of the Simple Ocean Data Assimilation (SODA) (Carton and Giese, 2008), and for the biogechemical variables from a Community Earth System Model (CESM) climatological model product (Moore et al., 2013). The model is forced at the surface with climatological winds from QuikSCAT (Risien and Chelton, 2008) and heat and freshwater surface fluxes from the Comprehensive Ocean-Atmosphere Data Set (COADS) (Da Silva et al., 1994). We used a fixed atmospheric $p\mathrm{CO}_2$ of 370 ~~μatm~~ μatm without CO_2 incrementation throughout the years and without seasonal variations. Starting from rest we ran the model for 8 years and used a climatology from years 5 through 8 for our analyses.

~~Since we are mostly concerned with climatological analysis, we chose not to represent processes such as river run-off and tides , which can be locally important.Nevertheless, the~~ Even though some processes as river runoff and tides are locally relevant (i.e., la Plata River, and Patagonia shelf), we are not considering them in the present study (see conclusions section). The low salinity waters from the La Plata river are ~~indirectly included as the model nudges to climatological salinity values in the region. However, our modeldoes not include river inputs of carbon, which is known to be an important factor regulating~~ included in the climatological forcing from COADS which are "nudged" into the model. These shortcomings may effect the results in some regions, but it is unlikely that they will affect the overall $p\mathrm{CO}_2$ ~~(Bauer et al., 2013). The lack of tides may adversely affect our model results in the inner shelf of Patagonia, where tidal amplitudes reach up to 12 meters at some points (Kantha, 1995; Saraceno et al., 2010) and tidal fronts are known to impact oceanic $p\mathrm{CO}_2$ (Bianchi et al., 2005). Despite these local shortcomings our model results should not be significantly affected in the overall climatological estimates of the parameters and processes controlling $p\mathrm{CO}_2$ in our domain.These processes will be implemented in future studies.~~results in the wider domain.

2.2 Analysis

Ocean surface $p\mathrm{CO}_2$ is the most important variable determining the air-sea CO_2 flux. This is because the variability of ocean $p\mathrm{CO}_2$ is much greater than that of atmospheric $p\mathrm{CO}_2$, and variations in the gas transfer coefficient are usually several times smaller than those of ~~surface ocean~~ ocean surface $p\mathrm{CO}_2$ (Takahashi et al., 2002). Seawater $p\mathrm{CO}_2$ is regulated by the concentration of dissolved inorganic carbon (DIC), alkalinity (ALK), temperature (T) and salinity (S). While T and S are controlled solely by physical factors, DIC and ALK are affected both by biological production and physical transport. DIC concentration is also affected by air-sea CO_2 fluxes (Sarmiento and Gruber, 2006).

In our model, ~~surface ocean~~ ocean surface $p\mathrm{CO}_2$ is calculated through a full model implementation of the seawater inorganic carbon system, i.e., as a function of the state variables T, S, DIC, and ALK, with the dissociation constants k_1 and k_2 from Millero (1995). In order to assess the impact of different parameters on $p\mathrm{CO}_2$ variability, we decompose $p\mathrm{CO}_2$ with respect to T, S, DIC and ALK, following the approach of ~~Lovenduski et al. (2007); Doney et al. (2009); Turi et al. (2014); Signorini et al. (2013)~~Lovenduski et al. (Signorini et al. (2013),

$$\Delta pCO_2 = \frac{\partial pCO_2}{\partial DIC}\Delta DIC^s + \frac{\partial pCO_2}{\partial ALK}\Delta ALK^s + \frac{\partial pCO_2}{\partial T}\Delta T + \frac{\partial pCO_2}{\partial FW}\Delta FW \quad (1)$$

,

where the Δ's are anomalies, either spatial or temporal, relative to a domain or an annual mean, respectively. DIC^s and ALK^s are the variable concentrations normalized to a domain-averaged surface salinity of 34.66. ~~The~~ , therefore effects from dilution of DIC and ALK through freshwater input are not included in DIC^s and ALK^s terms. The dilution effect is considered instead in the freshwater component (FW) ~~is calculated in order to include~~ as it includes the effects of precipitation and evaporation on DIC and ALK concentrations.

The partial derivatives were calculated following Doney et al. (2009). $p\mathrm{CO}_2$ was recalculated four times adding a small perturbation to the spatial, or temporal, domain average for each variable (T, S, DIC, ALK) while maintaining the other 3 variables fixed to the domain averaged surface values. The perturbation applied here was 0.1% of the domain mean.

In order to investigate the parameters and processes controlling $p\mathrm{CO}_2$ on the continental margin, we limited our temporal analysis to three regions with depths shallower than 1000 m: the Southeast Brazilian Shelf (SEBS) in the northern part of the domain, the South Brazilian Shelf (SBS) in the

middle of the domain that encompasses the Uruguayan Shelf, and the ~~Patagonian~~ Patagonia Shelf (PS) to the south of the domain (Fig.1a). We also selected two open ocean regions for comparison with the continental shelves: a subtropical (ST) and a subantarctic (SA) region (Fig.1b). In each of these regions, we estimated the monthly contribution of each parameter to the modeled $p\mathrm{CO}_2$ variability by spatially averaging the parameters within each region, and using the temporal anomalies (subtracting the annual ~~average~~mean) on Eq. 1. For the spatial analysis, we used the whole study area and then calculated in each grid cell the spatial anomalies (subtracting the domain mean of that grid cell), finally applying it ~~on~~ to Eq. 1.

In order to identify the main processes responsible for the variability of surface $p\mathrm{CO}_2$, we used a progressive series of sensitivity experiments as in Turi et al. (2014), focusing on the processes of biological production, CO_2 solubility, air-sea CO_2 fluxes, and physical transport. To quantify these processes, we made three additional model runs, progressively excluding each process. In the first experiment (E1), we set the CO_2 gas exchange flux coefficient between the atmosphere and the ocean to zero, inhibiting gas exchange in the surface layer. In the second experiment (E2), we started from E1 and also turned off the ~~photosynthetic~~ photosynthetically available radiation (PAR), preventing phytoplankton growth. Finally, in experiment E3, the CO_2 solubility was set to a constant value, calculated with the domain-averaged surface salinity and temperature of 34.66 and 12.33 ~~°C~~°C, respectively, while maintaining the changes of E1 and E2. The control run minus E1 represents the impact of gas exchange between ocean and atmosphere, E1 minus E2 represents the impact of biology, E2 minus E3 represents the impact of variable solubility. The last experiment (E3), in which there is no air-sea flux, no biology and constant solubility represents the impact of physical transport (Turi et al., 2014).

Given the short model integration times, the vertical gradients in the E3 simulation have not come in to steady-state with the processes. So our physical transport is working on the vertical DIC gradients established by the biological pump. Since the lateral boundary conditions are the same for all experiments, these simulations are therefore only approximations of the impact of each process on $p\mathrm{CO}_2$. Further, this separation assumes a linear additionality of each process, which is clearly a strong simplification given the non-linear nature of the inorganic carbonate system (Sarmiento and Gruber, 2006). The same spatial and temporal analysis described for the variables (ALK, DIC, T and FW) was also applied for the processes experiments (air-sea CO_2 flux, biology, CO_2 solubility, physical transport).

3 Model Evaluation and Validation

Model results were evaluated against data from the Surface Ocean CO_2 Atlas (SOCAT) version 2 (Bakker et al., 2013). SOCAT fCO_2 observations were converted into $p\mathrm{CO}_2$ using the set of equations from Körtzinger (1999) and then compared with modeled $p\mathrm{CO}_2$ to assess the overall skill of the model. Due to the paucity of in-situ observations, particularly on the continental shelves, we used monthly climatologies for the comparison. The seasonal model evaluation was made over the whole domain (Fig.1). On the Patagonia Shelf, data from the Argentinian cruises ARGAU and GEF3 were used for a more focused comparison of the model results (Bianchi et al., 2009). For the Brazilian continental shelves no data were found for local comparisons.

Overall, our model ~~represents~~ simulates reasonably well the seasonality of ocean surface $p\mathrm{CO}_2$, with the latitudinal and cross-shelf gradients represented during all seasons (Fig.2). Since our simulation has a fixed atmospheric $p\mathrm{CO}_2$ of 370 ~~μatm~~μatm, this value separates the source from the sink regions. In the northernmost oceanic region, between ~~$16°S$ and $30°S$~~16°S and 30°S, the observations show $p\mathrm{CO}_2$ close to $370 - 380$ ~~μatm~~μatm. Therefore this region acts as a weak source of CO_2 to the atmosphere. This tendency is well captured by the model, particularly during summer and autumn. From ~~$30°S$ to $55°S$~~30°S to 55°S, the whole offshore region acts as a CO_2 sink, with $p\mathrm{CO}_2$ ranging from ~~250μatm~~ 250 μatm to 350 ~~μatm~~ μatm during all seasons in the model results. The observations show the same pattern down to ~~$50°S$~~50°S. However in the southernmost region the observed $p\mathrm{CO}_2$ rises to values close to 400 ~~μatm~~μatm. On the Southeast Brazilian Shelf, there ~~was~~ were no data for model evaluation, but the overall behaviour of $p\mathrm{CO}_2$ agrees with previous results from Ito et al. (2005), who suggested that the continental shelf in this region acts as a source to the atmosphere ~~from inner to outer shelf~~ across both inner and outer shelves during all seasons. The southernmost and northernmost regions are where our model has the largest biases, underestimating the ocean surface $p\mathrm{CO}_2$. These biases could be due to a variety of reasons, including the high variability of the Antarctic Circumpolar Current and/or proximity to the model boundary with potential biases in the lateral boundary conditions used to force the model.

On the Patagonia Shelf the model was evaluated using in-situ observations from Bianchi et al. (2009) during the years 2000 to 2006 (Fig.3). The model agrees very well with the seasonality of the observations of this shelf region, in particular the high $p\mathrm{CO}_2$ values along the inner shelf, ~~characterizing these regions as~~ which make these regions a source of CO_2 during all seasons, but more intense during autumn/winter (Fig.3 b,c,f,g). In the mid-outer shelf the ocean generally acts as a sink, while to the north the ocean is in equilibrium with the atmosphere particularly during winter.

The monthly analysis was restricted to three offshore areas (A1, A2 and A3 in Fig.4a). We compared the spatial monthly mean modeled surface $p\mathrm{CO}_2$ with the monthly average of the SOCAT

pCO_2 data available in each area. Within these areas, we applied the following statistical indicators used in Dabrowski et al. (2014) in order to quantitatively assess model skill: model efficiency ~~(ME)~~ $ME = 1 - (\Sigma(O-M)^2)/(\Sigma(O-\bar{O})^2)$ (Nash and Sutcliffe, 1970), cost function ~~(CF)~~ $CF = (\Sigma \mid M-O \mid)/(n\sigma_o)$ (Ospar et al., 1998) and percentage of bias ~~(PB) (Allen et al., 2007)~~ $PB = \mid (\Sigma(O-M).100)/\Sigma O \mid$ (Allen et al., 2007), where M stands for modeled pCO_2 and O for observations from SOCAT database, n is the number of observations and σ_o is the standard deviation of all observations. These statistics are indicators of the model's performance and provide complementary information of the model skill~~(Dabrowski et al., 2014). Basically,~~ . ME relates model error with observational variability, CF is the ratio of mean absolute error to standard deviation of observations, and PB is the bias normalized by the observations (Dabrowski et al., 2014; Stow et al., 2009). Basically if $ME > 0.5$, $CF < 1$ and $PB < 20$, indicate that the model is "~~excellent/good~~good/reasonable "when comparing to observations. If $ME < 0.2$, $CF > 3$ and $PB > 40$ the model is classified as "poor/bad ".

Modeled pCO_2 results for A1 agree very well with the observations, representing the pCO_2 evolution throughout the year with maximum values in summer (Fig.4b). All statistical indicators characterized the model with a good/reasonable skill in A1 (Table 1).

A2 is the region with the largest pCO_2 standard deviation from both model and observations (Fig.4c). This region is near the confluence between the warm Brazil Current and the cold Malvinas Current, generating one of the most energetic regions of the world's oceans. Moreover, this region comprises the shelfbreak front, with differences in stratification, local dynamics and salinity between shelf waters and Malvinas current waters (Fig.2a). Consequently, ME was estimated as poor/bad in this region, probably due to the high pCO_2 data variability. But CF and PB were both rated as "good/reasonable~~/good~~"(Table 1).

In A3 the model consistently underestimated pCO_2 (Fig.4d). This bias is seen in the seasonal comparison and in the monthly analysis, where summer is the only season for which ~~modelled~~ modeled pCO_2 is within the standard deviation of the observations. ME was estimated as poor/bad in A3, but PB and CF rated our model as reasonable and good, respectively. (Table 1). Both A2 and A3 regions are close to an area of elevated eddy kinetic energy (Fig.4a), which could explain the large standard deviation and biases in these regions.

The Taylor diagram is consistent with the model efficiency (ME) estimate, showing good/reasonable results in A1, with a correlation of 0.8, and poor results in A2 and A3, with negative correlations (Fig.5). Only in A1, the correlation was found to be statistically significant. Aside from greater pCO_2 variability in these regions, the poor results found in A2 and A3 could also be due to the paucity of

the observational data both in space and time.

Furthermore, in order to validate the baseline of our model, seasonal climatologies of modeled sea surface temperature and chlorophyll-a were compared with climatologies from AVHRR and MODIS-aqua, respectively. Results and a detailed discussion of this validation are shown in the appendix.

In conclusion, our model reproduces ~~satisfyingly~~ the most important north-south and inner-outer shelf gradients seen in the $p\mathrm{CO}_2$ observations. ~~We now proceed to estimate the~~ While there is clearly room for improvement, we deem this level of agreement as sufficient for proceeding to the analysis of the processes and parameters affecting $p\mathrm{CO}_2$ variability in this region.

4 Results and Discussion

4.1 $p\mathrm{CO}_2$ drivers - spatial analysis

Modeled $p\mathrm{CO}_2$ spatial anomalies relative to the domain average are shown in Fig.5a, with positive anomalies prevailing on the Brazilian continental shelves, inner-mid Patagonia Shelf and North of ~~$32°S$~~32°S, while the negative anomalies are found in the open ocean south of ~~$32°S$~~ 32°S and in the mid-outer Patagonia Shelf. DIC^s has the highest impact on the spatial variations, being counteracted by ALK^s and T ~~.(Fig.5~~(Fig.6). In contrast, the fresh water flux has a minor influence on the spatial anomalies of $p\mathrm{CO}_2$, agreeing with Turi et al. (2014) and Doney et al. (2009). ~~After T and DIC^s, ALK has the larger~~ Even though with a smaller role, ALK^s influence on $p\mathrm{CO}_2$ anomalies ~~, with~~ presented absolute values higher (-100 to 100 ~~μatm~~μatm) than previous studies in other regions (Lovenduski et al., 2007; Turi et al., 2014). The higher contribution of both ~~DIC and ALK~~ DIC^s and ALK^s to the spatial variations in $p\mathrm{CO}_2$ could be explained by the more heterogeneous domain that encompasses several distinct surface water masses and frontal zones. Also, ~~this~~ the elevated contribution of ~~ALK~~ ALK^s could be due to our relatively high ~~$CaCO_3$~~ CaCO_3 to biological production ratio of 0.07.

The changes in the state variables affecting $p\mathrm{CO}_2$ are ultimately being driven by physical and biogeochemical processes~~, we thus investigate which of these processes control~~. We investigate the role of each of these processes in controlling the changes in surface $p\mathrm{CO}_2$ from our sensitivity experiments (E1, E2, E3). The most important processes affecting the spatial distribution of $p\mathrm{CO}_2$ ~~spatial distribution~~ are biological production (E1 - E2) and physical transport (E3) (Fig.~~6~~7). When physical transport (vertical and horizontal) is the only process altering $p\mathrm{CO}_2$, we observe an increase in $p\mathrm{CO}_2$ of up to ~~800μatm~~ 800 μatm on the continental shelves, due to the upwelling and vertical mixing

of DIC-rich subsurface waters. At the same time, the effect of biological production on the uptake of DIC and changes in ALK due to nitrate uptake and production/dissolution of ~~$CaCO_3$~~ $CaCO_3$ accounts for a decrease of up to ~~$-600\mu atm$~~ -600 μatm on the continental shelves. Solubility effects (E2 - E3) are responsible for a decrease in $p\mathrm{CO}_2$ south of ~~$45°S$~~ 45°S and an increase in $p\mathrm{CO}_2$ to the north, ranging from -50 to ~~$50\mu atm$~~50 μatm. Finally, air-sea CO_2 fluxes (Control - E1) have little impact on regulating the ocean surface $p\mathrm{CO}_2$. The effect of both biological production and physical transport is maximal on the continental shelves, with the balance between these processes largely controlling $p\mathrm{CO}_2$ ~~. On~~ there. In the open ocean, physical transport largely controls $p\mathrm{CO}_2$, again being counteracted by biological production. North of ~~$45°S$~~45°S, biological production is being counteracted by physical transport and solubility, whereas to the south of ~~$45°S$~~ 45°S physical transport is being counteracted by biological production and solubility.

The strong effect of biological production on the shelf region is a result of the elevated nutrient supply and high primary production found in these regions, with increasing contribution towards the inner shelves. Physical transport presents a higher contribution on the continental shelves, where the mixed layer often spans the entire water column, showing the importance of vertical mixing in bringing metabolic DIC as well as nutrients to the surface waters, therefore increasing $p\mathrm{CO}_2$. These results are in agreement with previous studies (c.f. Turi et al. (2014)), showing the importance of the biological net community production and advection of ALK and DIC (physical transport) in controlling ocean surface $p\mathrm{CO}_2$. This suggests a major role of net community production in reducing ocean $p\mathrm{CO}_2$ in the region.

4.2 $p\mathrm{CO}_2$ drivers - temporal analysis

In order to identify the seasonal variability of the contribution of each parameter, we used local grid temporal anomalies over the seasonal cycle (Fig. ~~7~~8). DIC^s and T are still the most influential parameters, with increasing importance on the continental shelves. The contribution by ALK^s ~~appears~~ is relevant only on continental shelves south of 32°~~S~~S, and FW ~~is~~ have a minor influence (not shown). It is important to highlight that the magnitude of the signals seen in this analysis is one order of magnitude smaller than the previous spatial analysis. ~~Thus, the high absolute contributions found in the spatial analysis are~~ This is likely due to our large and heterogeneous domain, which results in much spatial gradients than what is modeled over the seasonal cycle.

The contribution of the state variables in each continental shelf region (Fig. ~~8~~9) shows that these three regions have distinct characteristics, with different contributions from each parameter. In all three regions, DIC^s and T are the most important parameters affecting $p\mathrm{CO}_2$ anomalies, albeit with opposing and seasonally varying contributions. While in summer the T contribution increases

pCO_2, that of ~~DIC~~ DIC^s acts to diminish pCO_2. The opposite occurs in winter. The Southeast Brazilian Shelf (SEBS) is the region with the least variability in pCO_2 anomalies, with the contributions of both DIC^s and T in this region ranging from ~~$-10\mu atm$ to $10\mu atm$~~ -10 μatm to 10 μatm.

The South Brazilian Shelf (SBS) is the region with the largest variability in pCO_2 anomalies, with ALK^s having the most prominent impact on pCO_2 ~~when~~ compared to the other regions - up to ~~$15\mu atm$~~ 15 μ atm in spring. DIC^s is the most important parameter in this area, with a contribution of up to ~~$70\mu atm$~~70 μ atm, followed by temperature, with a contribution of up to ~~$60\mu atm$~~ 60 μatm in the winter. On the Patagonia Shelf (PS) and South Brazilian Shelf (SBS), although the amplitude of the contributions by DIC^s and T are large, the tendency of these two terms to cancel each other out results in smaller pCO_2 anomalies. In both SBS and PS, pCO_2 is predominately controlled by T and DIC^s, with small contributions from ALK and FW.

Seasonal warming/cooling is largely controlling pCO_2 anomalies signals throughout the continental shelves, only being dampened by DIC^s, and also by ALK^s in the case of the South Brazilian Shelf (SBS). This pattern of seasonal variation of the parameters on continental shelves agrees with the results from ~~Signorini et al. (2013); Turi et al. (2014)~~Signorini et al. (2013) and Turi et al. (2014), although with different absolute values. ~~Also the~~ The pattern of diminishing variability towards subtropical continental shelves is also shown by Signorini et al. (2013).

This pattern of opposing contributions of T and DIC was also found along the North American east coast by Signorini et al. (2013), who attributed winter mixing and the spring-summer biological drawdown as the processes responsible for pCO_2 and DIC variability. In the offshore subtropical region (ST) the pCO_2 anomalies have higher ~~amplitude~~ amplitudes than in the adjacent continental shelf (SEBS), and are driven mainly by Temperature, with the other variables having minor contributions (Fig.~~10~~.11). In the offshore southern region (SA), ~~DIC~~ DIC^s controls pCO_2 variability, with ~~T and ALK~~ T and ALK^s dampening pCO_2 anomalies (Fig.~~9~~.10), similar to the adjacent shelf (PS).

The analysis of the processes underlying this seasonal variability using our progressive sensitivity simulations ~~show~~ shows that on all shelf regions, biological production and CO_2 solubility mostly control pCO_2 variability (Fig.~~9~~.10). Physical transport, although weaker than biological production, acts to diminish the pCO_2 variability by counteracting the effects of biology and increasing DIC concentrations. In our case, physical transport controls pCO_2 spatially, but the temporal effects of physical transport are much weaker than in Turi et al. (2014) along the California coast. This is probably because the much stronger upwelling in that region acts to dampen the effects of biology by bringing DIC rich waters to the surface. Along western boundaries, upwelling is weaker and

more localized. Physical transport is therefore more related to processes that modulate vertical mixing and stratification, thereby controlling the seasonal enrichment of surface waters, and horizontal advection due to the presence of two major western boundary currents. Finally, air-sea CO_2 fluxes are only a minor contribution to the pCO_2 anomalies.

In conclusion, on the Patagonia Shelf (PS), the biological production is the most important contributor to pCO_2 variability, with a peak summer contribution of ~~$-80 \mu atm$~~ -80 μatm and a maximum in the winter of ~~$70 \mu atm$~~ 70 μatm. On the South Brazilian Shelf (SBS), solubility is the most influential process (up to ~~$90 \mu atm$~~ 90 μatm), followed by biological production and physical transport, during all seasons. On the Southeast Brazilian Shelf (SEBS), the pattern is the same as in the SBS, although with a smaller magnitude and variability. Physical transport, although large in absolute contributions in the spatial analysis, has a lower contribution to pCO_2 variability in the temporal analysis.

In the subtropical region, processes that control ~~pCO2~~ the temporal variability of pCO_2 on the shelf and offshore are different. In the open ocean (ST) (Fig~~.10~~.11) pCO_2 is mainly controlled by solubility, with the biological production having the least effect on pCO_2. This contrasts with the importance of biology on mid/low latitude continental shelves (SEBS). In the subantarctic region, the processes controlling pCO_2 are similar for both the offshore region (SA) and the adjacent continental shelf (PS) (Fig.9). In this case biological production is the most important process being countered mainly by solubility, although with a smaller magnitude in the offshore region.

4.3 Air-sea CO_2 fluxes

On the continental margins, we investigate monthly averaged air-sea CO_2 fluxes on the inner shelf (0-100 meters depth), mid-outer shelf (100-200 meters depth) and shelf break-slope (200-1000 meters depth). As shown in the previous sections, the inner shelves have a potential to act as a source of CO_2, while the mid/outer shelves tend to act as a sink of CO_2. On the ~~brazilian~~ Brazilian shelves (SBS and SEBS) the flux density of CO_2 in the inner shelves is around $0 - 0.5$ ~~$molCm^{-2}yr^{-1}$~~ molCm^{-2}yr^{-1}, thus characterizing this region as a weak source. On the mid/outer shelf these regions shift to sinks of CO_2, with a flux density of $-1 - 0$ ~~$molCm^{-2}yr^{-1}$~~ molCm^{-2}yr^{-1} on the Southeast Brazilian shelf (SEBS). On the mid/outer South Brazilian Shelf (SBS) the sink is slightly stronger with a average flux between -1.5 and -0.5 ~~$molCm^{-2}yr^{-1}$~~ molCm^{-2}yr^{-1} (Figs. ~~11a and 11b~~12a and 12b). The Patagonia Shelf (PS) acts on average as a sink of CO_2, with fluxes larger than on the Brazilian shelves. CO_2 absorption on PS intensifies from the inner shelf (-1.0 / -0.5 ~~$molCm^{-2}yr^{-1}$~~ molCm^{-2}yr^{-1}) to the outer shelf and continental slope (-2.0 / -4.0 ~~$molCm^{-2}yr^{-1}$~~ molCm^{-2}yr^{-1}) (Fig. ~~11c~~12c). Although, PS acts on average as a sink throughout the whole continental shelf, there are some coastal

regions that act as a source of CO_2, which agrees with the observations of Bianchi et al. (2009).

Annual ~~averaged modelled~~ mean modeled air-sea CO_2 fluxes agreed reasonably well with global climatologies in the oceanic regions (not shown) (Takahashi et al., 2002; Landschützer et al., 2014). South of ~~$30°S$~~30°S, the open ocean acts on average as a sink of atmospheric CO_2, absorbing up to ~~$4 mol C m^{-2} yr^{-1}$~~4 molCm^{-2}yr^{-1}. North of ~~$30°S$~~30°S, the open ocean is on average in equilibrium with the atmosphere (Fig.11). On the continental margins, our annual ~~averaged~~ mean air-sea CO_2 fluxes ~~compares~~ compare well with the global estimate from Laruelle et al. (2014), where the ~~Patagonian~~ Patagonia Shelf acts as a sink of CO_2 (-1.0 to ~~$-4.0 mol C m^{-2} yr^{-1}$~~$-3.0$ molCm^{-2}yr^{-1}) and the Brazilian shelves act as ~~a week source~~ weak sources of CO_2 (0 to 1 ~~$mol C m^{-2} yr^{-1}$~~molCm^{-2}yr^{-1}). Nevertheless, we found variability on each continental shelf, with regions on the inner Patagonia Shelf acting as a source or in equilibrium with the atmosphere (0 to 2.0 ~~$mol C m^{-2} yr^{-1}$~~molCm^{-2}yr^{-1}), and regions on the outer Brazilian shelves acting as ~~a sink~~ sinks of CO_2.

4.4 Vertical Structure - Case Study at Argentine OOI Site

Seasonal variations in mixing and stratification control the evolution of the mixed layer depth and consequently the vertical structure of the state variables of the carbonate system. Diapycnal fluxes of DIC and DIC sinks from primary production are important processes regulating ocean surface pCO_2 (Rippeth et al., 2014). Therefore, the mixed layer depth is linked with the surface pCO_2 variability.

In order to understand the seasonal evolution of the upper ocean vertical distribution of the state variables in the region and how it affects surface pCO_2, we chose the location of the Ocean Observatory Initiative (OOI) site in the Argentine Basin at ~~$42°S, 42°W$~~42°S, 42°W (Fig.1 a), as it will soon become a test-bed for the validation of biogeochemical models globally and regionally. We extracted modeled climatological vertical profiles of DIC concentration, temperature and chlorophyll-a, and compared with the ~~modelled~~ modeled surface pCO_2 and mixed layer depth (Fig.~~12~~13).

During the entire year, this location acts in our model as a sink for atmospheric CO_2, with ~~modelled~~ modeled surface pCO_2 ranging from ~~$280 \mu atm$ to $320 \mu atm$~~280 μatm to 320 μatm. The contribution of DIC^s and T are again driving surface pCO_2 anomalies. In this case DIC^s is controlling the anomalies signal, being dampened by temperature. The main processes affecting pCO_2 in this location is biological production and solubility. Minimum pCO_2 in summer coincides with strong stratification and elevated subsurface biological production, respectively, with the opposing contribution of DIC^s and T leading to pCO_2 anomalies near zero. Maximum pCO_2 occurs when the mixed layer depth deepens, during fall and winter, when vertical mixing cause an increase in

the concentration of DIC in the surface waters. This affects $p\mathrm{CO}_2$ much more than the decrease in temperature, resulting in positive $p\mathrm{CO}_2$ anomalies. After winter, this excess of DIC is consumed by biological fixation during spring and summer, thus reducing surface $p\mathrm{CO}_2$.

5 Conclusions

In this study, we used a regional ~~hydrodynamical model coupled with~~ hydrodynamic model coupled to a biogeochemical model to investigate, in a climatological sense, the main parameters and processes that control ocean surface $p\mathrm{CO}_2$ and air-sea CO_2 fluxes in the southwestern Atlantic Ocean. Modeled ocean surface $p\mathrm{CO}_2$ compared well with the available in-situ data, reproducing the expected meridional and cross-shelf gradients of $p\mathrm{CO}_2$, with elevated $p\mathrm{CO}_2$ in the inner shelves and at lower latitudes. Our results highlight that the most important variables controlling the spatio-temporal variability of $p\mathrm{CO}_2$ are T and ~~DIC~~DIC^s. These two variables have opposing effects on $p\mathrm{CO}_2$ and have been shown to be the main drivers of $p\mathrm{CO}_2$ both in global (Sarmiento and Gruber, 2006; Doney et al., 2009) and in other regional studies (Turi et al., 2014; Signorini et al., 2013; Lovenduski et al., 2007). Following ~~DIC~~ DIC^s and T, we found that ~~ALK is an~~ ALK^s is a secondarily important spatial regulator of $p\mathrm{CO}_2$, with increasing importance on the South brazilian Shelf (SBS) and in the southern open ocean region (SA).

The most important processes underlying changes on the state variables and thus on $p\mathrm{CO}_2$ are biological production and CO_2 solubility. Biological production is particularly important on the continental shelves , with higher contribution in shelf regions at high latitudes. ~~On~~ In the open ocean, CO_2 solubility is the main ~~processes~~ process driving $p\mathrm{CO}_2$ variations in the subtropics, while in the subantarctic both CO_2 solubility and biological production are important drivers of $p\mathrm{CO}_2$ variability.

The southwestern Atlantic Ocean acts, on average, as a sink of atmospheric CO_2 south of ~~30° S~~30°S, and is close to equilibrium to the north. In the inner continental shelves the ocean acts either as a weak source or is in equilibrium with the atmosphere. To the outer shelf the ocean ~~shifts~~ changes to a sink of CO_2. The entire Patagonian shelf ~~acts~~act, on average, as a sink, but there are some particular regions in the inner shelf that acts as a source of CO_2. The total integrated flux agrees well with Laruelle et al. (2014), particularly on the Brazilian Shelves (SEBS and SBS). However, in the Patagonia Shelf (PS), we found a slightly stronger sink on the mid/outer Patagonian Shelf (-1.0 to ~~$-4.0\ molC m^{-2} yr^{-1}$~~ -3.0 molCm^{-2}yr^{-1}) and more variability towards the inner shelf.

~~Modelling studies~~ Our model does not include river inputs of carbon, which are known to be an important factor regulating $p\mathrm{CO}_2$ (Bauer et al., 2013). The lack of tides may adversely affect

our model results in the inner shelf of Patagonia, where tidal amplitudes reach up to 12 meters at some points (Kantha, 1995; Saraceno et al., 2010) and tidal fronts are known to impact oceanic pCO_2 (Bianchi et al., 2005). In future regional studies focused on the Patagonia shelf, tides and river run-off should be included.

Modeling studies such as this one depend heavily on in-situ observations, the lack of which hampers our ability to properly refine our model~~, this~~. This will certainly be improved by future efforts of data assimilation of vertical profiles of biogeochemical and physical variables from the OOI site at the Argentine basin. ~~In future studies we will also add tides and river run-off to the model, hopefully diminishing the biases in the southernmost and La Plata regions. However, this~~ This study is a first step in understanding the processes controlling surface pCO_2 in an undersampled, yet highly important, region of the world's ocean. Improved understanding of the processes controlling the surface distribution of pCO_2 on continental shelves and in the open ocean is fundamental for quantifying the ocean's response to and its feedback on climate change.

Appendix A: Model Validation (SST and Chlorophyll-a)

Seasonal climatologies of 4 years of modeled sea surface temperature and chlorophyll-a concentration were compared with climatologies from the sensors AVHRR (1985-2002) and Modis-aqua (2003-2013), respectively (Figs. ~~13 and~~ 14 and 15). Modeled sea surface temperature compared well with AVHRR (Fig.~~13~~.14) representing both subantarctic and subtropical oceanic regions during all seasons.

Modeled chlorophyll-a concentration reproduces the general pattern from MODIS-aqua (Fig.~~14~~.15), with low concentrations in the oceanic regions and higher concentrations on the continental shelves. However, modeled chlorophyll-a concentrations are overestimated in the ~~oceanic~~ open ocean regions (0.5 ~~$mgChla-am^{-3}$~~ mgChla-am^{-3}), especially in the spring season (up to 1 ~~$mgChla-am^{-3}$~~). ~~On~~ mgChla-am^{-3}). In the coastal regions, we underestimate chlorophyll-a on the Patagonia Shelf during spring and summer seasons. Expectedly, there was an underestimation in the La Plata region, since we are not modeling the nutrient and organic loads from the river. Finally, on the Brazilian shelf our model overestimates chlorophyll-a, particularly during summer and spring seasons. These biases may be due to our application of a relatively simple ecosystem model with only one phytoplankton functional type in such a wide region, which encompasses several ecological provinces. Nevertheless, the general pattern is well reproduced in this first effort in modeling the biogeochemistry of the southwestern Atlantic Ocean, and the biases may not significantly compromise our analysis of

drivers and processes ~~on~~ of pCO_2 variability.

Acknowledgements. PHRC acknowledges support from the Brazilian agencies Conselho Nacional de Desenvolvimento Científico e Tecnológico (CNPq), grants 483112/2012-7 and 307385/2013-2, and the ~~Fundacão de Amparo a Pesquisa do Estado do Rio Grande do Sul (FAPERGS), grant 2166~~Coordenação de Aperfeiçoamento de Pessoal de Nível Superior (CAPES Process 23038.004299/~~12-8~~2014-53). RA acknowledges support from a CAPES scholarship. SCD and IDL acknowledge support from the National Science Foundation (NSF AGS-1048827). NG and GT received support from ETH Zurich and from the EU FP7 project CarboChange (264879).

The Surface Ocean CO_2 Atlas (SOCAT) is an international effort, supported by the International Ocean Carbon Coordination Project (IOCCP), the Surface Ocean Lower Atmosphere Study (SOLAS), and the Integrated Marine Biogeochemistry and Ecosystem Research program (IMBER), to deliver a uniformly quality-controlled surface ocean CO_2 database. The many researchers and funding agencies responsible for the collection of data and quality control are thanked for their contributions to SOCAT.

We are greatly indebted with the Ministero de Defensa de Argentina that supported the project "Balance y variabilidad del flujo mar-aire en el Mar Patagónico"(PIDDEF 47/11). This work was carried out with the aid of a grant from the Inter-American Institute for Global Change Research (IAI) CRN3070 which is supported by the US National Science Foundation (Grant GEO-1128040).

Supported by Global Environmental Facilities (GEF) in the frame of PNUD ARG/02/018-GEF BIRF N° 28385-AR, subproject B-B46, and by Servicio de Hidrografía Naval. Additional support was provided by the ARGAU Project, Instituto Antártico Argentino, Institut National de Sciences de l'Univers, Processus Biogeochimiques dans l'Océan et Flux, Université Pierre et Marie Curie.

References

Allen, J., Somerfield, P., and Gilbert, F.: Quantifying uncertainty in high-resolution coupled hydrodynamic-ecosystem models, Journal of Marine Systems, 64, 3–14, doi:10.1016/j.jmarsys.2006.02.010, http://linkinghub.elsevier.com/retrieve/pii/S0924796306001035, 2007.

Bakker, D. C. E., Pfeil, B., Smith, K., Hankin, S., Olsen, a., Alin, S. R., Cosca, C., Harasawa, S., Kozyr, a., Nojiri, Y., O'Brien, K. M., Schuster, U., Telszewski, M., Tilbrook, B., Wada, C., Akl, J., Barbero, L., Bates, N., Boutin, J., Cai, W.-J., Castle, R. D., Chavez, F. P., Chen, L., Chierici, M., Currie, K., de Baar, H. J. W., Evans, W., Feely, R. a., Fransson, a., Gao, Z., Hales, B., Hardman-Mountford, N., Hoppema, M., Huang, W.-J., Hunt, C. W., Huss, B., Ichikawa, T., Johannessen, T., Jones, E. M., Jones, S. D., Jutterström, S., Kitidis, V., Körtzinger, a., Landschtzer, P., Lauvset, S. K., Lefèvre, N., Manke, a. B., Mathis, J. T., Merlivat, L., Metzl, N., Murata, a., Newberger, T., Ono, T., Park, G.-H., Paterson, K., Pierrot, D., Ríos, a. F., Sabine, C. L., Saito, S., Salisbury, J., Sarma, V. V. S. S., Schlitzer, R., Sieger, R., Skjelvan, I., Steinhoff, T., Sullivan, K., Sun, H., Sutton, a. J., Suzuki, T., Sweeney, C., Takahashi, T., Tjiputra, J., Tsurushima, N., van Heuven, S. M. a. C., Vandemark, D., Vlahos, P., Wallace, D. W. R., Wanninkhof, R., and Watson, a. J.: An update to the Surface Ocean CO_2 Atlas (SOCAT version 2), Earth System Science Data Discussions, 6, 465–512, doi:10.5194/essdd-6-465-2013, http://www.earth-syst-sci-data-discuss.net/6/465/2013/, 2013.

Bauer, J. E., Cai, W.-J., Raymond, P. a., Bianchi, T. S., Hopkinson, C. S., and Regnier, P. a. G.: The changing carbon cycle of the coastal ocean., Nature, 504, 61–70, doi:10.1038/nature12857, http://www.ncbi.nlm.nih.gov/pubmed/24305149, 2013.

Bianchi, A. A., Piola, A. R., Pino, D. R., Schloss, I., Poisson, A., and Balestrini, C. F.: Vertical stratification and air-sea CO 2 fluxes in the Patagonian shelf, Journal of Geophysical Research, 110, C07 003, doi:10.1029/2004JC002488, http://doi.wiley.com/10.1029/2004JC002488, 2005.

Bianchi, A. a., Pino, D. R., Perlender, H. G. I., Osiroff, A. P., Segura, V., Lutz, V., Clara, M. L., Balestrini, C. F., and Piola, A. R.: Annual balance and seasonal variability of sea-air CO 2 fluxes in the Patagonia Sea: Their relationship with fronts and chlorophyll distribution, Journal of Geophysical Research, 114, C03 018, doi:10.1029/2008JC004854, http://doi.wiley.com/10.1029/2008JC004854, 2009.

Cai, W.-J.: The role of marsh-dominated heterotrophic continental margins in transport of CO 2 between the atmosphere, the land-sea interface and the ocean, Geophysical Research Letters, 30, 1849, doi:10.1029/2003GL017633, http://doi.wiley.com/10.1029/2003GL017633, 2003.

Carton, J. A. and Giese, B. S.: A reanalysis of ocean climate using Simple Ocean Data Assimilation (SODA), Monthly Weather Review, 136, 2999–3017, 2008.

Chen, C.-T. a., Huang, T.-H., Chen, Y.-C., Bai, Y., He, X., and Kang, Y.: Air-sea exchanges of CO_2 in world's coastal seas, Biogeosciences Discussions, 10, 5041–5105, doi:10.5194/bgd-10-5041-2013, http://www.biogeosciences-discuss.net/10/5041/2013/, 2013.

Ciais, P., Sabine, C., Bala, G., Bopp, L., Brovkin, V., Canadell, J., Chhabra, A., DeFries, R., Galloway, J., Heimann, M., et al.: Carbon and other biogeochemical cycles, in: Climate Change 2013: The Physical Science Basis. Contribution of Working Group I to the Fifth Assessment Report of the Intergovernmental Panel on Climate Change, pp. 465–570, Cambridge University Press, 2014.

Da Silva, A., Young, C., and Levitus, S.: Atlas of surface marine data 1994, vol. 1, algorithms and procedures, NOAA Atlas NESDIS 6, US Department of Commerce, NOAA, NESDIS, USA, p. 74, 1994.

Dabrowski, T., Lyons, K., Berry, A., Cusack, C., and Nolan, G. D.: An operational biogeochemical model of the North-East Atlantic: Model description and skill assessment, Journal of Marine Systems, 129, 350–367, doi:10.1016/j.jmarsys.2013.08.001, http://linkinghub.elsevier.com/retrieve/pii/S0924796313001711, 2014.

Doney, S. C., Lima, I., Feely, R. a., Glover, D. M., Lindsay, K., Mahowald, N., Moore, J. K., and Wanninkhof, R.: Mechanisms governing interannual variability in upper-ocean inorganic carbon system and air–sea CO2 fluxes: Physical climate and atmospheric dust, Deep Sea Research Part II: Topical Studies in Oceanography, 56, 640–655, doi:10.1016/j.dsr2.2008.12.006, http://linkinghub.elsevier.com/retrieve/pii/S096706450800427X, 2009.

Fennel, K. and Wilkin, J.: Quantifying biological carbon export for the northwest North Atlantic continental shelves, Geophysical Research Letters, 36, 2009.

Gonzalez-Silvera, A., Santamaria-del Angela, E., Garcia, V. M. T., Garcia, C. A. E., Millan-Nunez, R., and Muller-Karger, F.: Biogeographical regions of the tropical and subtropical Atlantic Ocean off South America: classification based on pigment (CZCS) and chlorophyll- a(SeaWiFS), Continental Shelf ..., 24, 983–1000, doi:10.1016/j.csr.2004.03.002, http://www.sciencedirect.com/science/article/pii/S0278434304000561, 2004.

Gruber, N.: Ocean biogeochemistry: Carbon at the coastal interface, Nature, 2015.

Gruber, N., Frenzel, H., Doney, S. C., Marchesiello, P., McWilliams, J. C., Moisan, J. R., Oram, J. J., Plattner, G.-K., and Stolzenbach, K. D.: Eddy-resolving simulation of plankton ecosystem dynamics in the California Current System, Deep Sea Research Part I: Oceanographic Research Papers, 53, 1483–1516, doi:10.1016/j.dsr.2006.06.005, http://linkinghub.elsevier.com/retrieve/pii/S0967063706001713, 2006.

Gruber, N., Lachkar, Z., Frenzel, H., Marchesiello, P., Münnich, M., McWilliams, J. C., Nagai, T., and Plattner, G.-K.: Eddy-induced reduction of biological production in eastern boundary upwelling systems, Nature Geoscience, 4, 787–792, doi:10.1038/ngeo1273, http://www.nature.com/doifinder/10.1038/ngeo1273, 2011.

Guerrero, R. A., Piola, A. R., Fenco, H., Matano, R. P., Combes, V., Chao, Y., James, C., Palma, E. D., Saraceno, M., and Strub, P. T.: The salinity signature of the cross-shelf exchanges in the Southwestern Atlantic Ocean: Satellite observations, Journal of Geophysical Research: Oceans, 119, 7794–7810, 2014.

Hauri, C., Gruber, N., Vogt, M., Doney, S. C., Feely, R. A., Lachkar, Z., Leinweber, A., McDonnell, A. M., Munnich, M., and Plattner, G.-K.: Spatiotemporal variability and long-term trends of ocean acidification in the California Current System, 2013.

Hofmann, E. E., Cahill, B., Fennel, K., a.M. Friedrichs, M., Hyde, K., Lee, C., Mannino, A., Najjar, R. G., O'Reilly, J. E., Wilkin, J., and Xue, J.: Modeling the Dynamics of Continental Shelf Carbon, Annual Review of Marine Science, 3, 93–122, doi:10.1146/annurev-marine-120709-142740, http://www.annualreviews.org/doi/abs/10.1146/annurev-marine-120709-142740, 2011.

Ito, R., Schneider, B., and Thomas, H.: Distribution of surface fCO2 and air–sea fluxes in the Southwestern subtropical Atlantic and adjacent continental shelf, Journal of Marine Systems, 56, 227–242, doi:10.1016/j.jmarsys.2005.02.005, http://linkinghub.elsevier.com/retrieve/pii/S0924796305000436, 2005.

Kantha, L.: Barotropic tides in the global oceans from a nonlinear tidal model assimilating altimetric tides: 1. Model description and results, Journal of Geophysical Research: Oceans (1978– ..., 100, 283–308, http://onlinelibrary.wiley.com/doi/10.1029/95JC02578/full, 1995.

Körtzinger, A.: Determination of carbon dioxide partial pressure (p (CO2)), Methods of Seawater Analysis, Third Edition, pp. 149–158, 1999.

Landschützer, P., Gruber, N., Bakker, D., and Schuster, U.: Recent variability of the global ocean carbon sink, Global Biogeochemical Cycles, 28, 927–949, 2014.

Laruelle, G. G., Dürr, H. H., Lauerwald, R., Hartmann, J., Slomp, C. P., Goossens, N., and Regnier, P. a. G.: Global multi-scale segmentation of continental and coastal waters from the watersheds to the continental margins, Hydrology and Earth System Sciences, 17, 2029–2051, doi:10.5194/hess-17-2029-2013, http://www.hydrol-earth-syst-sci.net/17/2029/2013/, 2013.

Laruelle, G. G., Lauerwald, R., Pfeil, B., and Regnier, P.: Regionalized global budget of the CO2 exchange at the air-water interface in continental shelf seas, Global biogeochemical cycles, 28, 1199–1214, 2014.

Lovenduski, N. S., Gruber, N., Doney, S. C., and Lima, I. D.: Enhanced CO 2 outgassing in the Southern Ocean from a positive phase of the Southern Annular Mode, Global Biogeochemical Cycles, 21, n/a–n/a, doi:10.1029/2006GB002900, http://doi.wiley.com/10.1029/2006GB002900, 2007.

Millero, F.: Thermodynamics of the carbon dioxide system in the oceans, Geochimica et Cosmochimica Acta, 59, 661–677, http://www.sciencedirect.com/science/article/pii/001670379400354O, 1995.

Moore, J. K., Lindsay, K., Doney, S. C., Long, M. C., and Misumi, K.: Marine ecosystem dynamics and biogeochemical cycling in the Community Earth System Model [CESM1 (BGC)]: Comparison of the 1990s with the 2090s under the RCP4. 5 and RCP8. 5 scenarios, Journal of Climate, 26, 9291–9312, 2013.

Muller-Karger, F. E., Varela, R., Thunell, R., Luerssen, R., Hu, C., and Walsh, J. J.: The importance of continental margins in the global carbon cycle, Geophysical Research Letters, 32, 2005.

Nash, J. and Sutcliffe, J.: River flow forecasting through conceptual models part I—A discussion of principles, Journal of hydrology, 10, 282–290, 1970.

Ospar, V. M., De Vries, I., Bokhorst, M., Ferreira, J., Gellers-Barkmann, S., Kelly-Gerreyn, B., Lancelot, C., Mensguen, A., Moll, A., Pätsch, J., Radach, G., Skogen, M., Soiland, H., Svendsen, E., and Vested, H. J.: Report of the ASMO modelling workshop on eutrophication Issues, 5–8 November 1996, OSPAR Commission Report, 102, 90, 1998.

Piola, A. and Matano, R.: Brazil and Falklands (Malvinas) currents, Ocean Currents: A Derivative of the Encyclopedia of Ocean Sciences, pp. 35–43, 2001.

Rippeth, T., Lincoln, B., Kennedy, H., Palmer, M., Sharples, J., and Williams, C.: Impact of vertical mixing on sea surface pCO2 in temperate seasonally stratified shelf seas, Journal of Geophysical Research: Oceans, 119, 3868–3882, 2014.

Risien, C. M. and Chelton, D. B.: A global climatology of surface wind and wind stress fields from eight years of QuikSCAT scatterometer data, Journal of Physical Oceanography, 38, 2379–2413, 2008.

Saraceno, M., D'Onofrio, E., Fiore, M., and Grismeyer, W.: Tide model comparison over the Southwestern Atlantic Shelf, Continental Shelf Research, 30, 1865–1875, doi:10.1016/j.csr.2010.08.014, http://linkinghub.elsevier.com/retrieve/pii/S0278434310002712, 2010.

Sarmiento, J. and Gruber, N.: Ocean biogeochemical dynamics, Princeton University Press, 2006.

Shchepetkin, A. and McWilliams, J.: The regional oceanic modeling system (ROMS): a split-explicit, free-surface, topography-following-coordinate oceanic model, Ocean Modelling, 9, 347–404, http://linkinghub.elsevier.com/retrieve/pii/S1463500304000484, 2005.

Signorini, S. R., Mannino, A., Najjar, R. G., Friedrichs, M. a. M., Cai, W.-J., Salisbury, J., Wang, Z. A., Thomas, H., and Shadwick, E.: Surface ocean p CO 2 seasonality and sea-air CO 2 flux estimates for the North American east coast, Journal of Geophysical Research: Oceans, 118, 5439–5460, doi:10.1002/jgrc.20369, http://doi.wiley.com/10.1002/jgrc.20369, 2013.

Stow, C. A., Jolliff, J., McGillicuddy, D. J., Doney, S. C., Allen, J. I., Friedrichs, M. A., Rose, K. A., and Wallhead, P.: Skill assessment for coupled biological/physical models of marine systems, Journal of Marine Systems, 76, 4–15, 2009.

Takahashi, T., Sutherland, S. C., Sweeney, C., Poisson, A., Metzl, N., Tilbrook, B., Bates, N., Wanninkhof, R., Feely, R. A., Sabine, C., Olafsson, J., and Nojiri, Y.: Global sea–air CO 2 flux based on climatological surface ocean p CO 2 , and seasonal biological and temperature effects, Deep Sea Research Part II: Topical Studies in Oceanography, 49, 1601–1622, 2002.

Takahashi, T., Sutherland, S. C., Wanninkhof, R., Sweeney, C., Feely, R. A., Chipman, D. W., Hales, B., Friederich, G., Chavez, F., Sabine, C., et al.: Climatological mean and decadal change in surface ocean pCO 2, and net sea–air CO 2 flux over the global oceans, Deep Sea Research Part II: Topical Studies in Oceanography, 56, 554–577, 2009.

Tsunogai, S., Watanabe, S., and Sato, T.: Is there a "continental shelf pump" for the absorption of atmospheric CO2?, Tellus B, 51B, 701–712, http://onlinelibrary.wiley.com/doi/10.1034/j.1600-0889.1999.t01-2-00010.x/abstract, 1999.

Turi, G., Lachkar, Z., and Gruber, N.: Spatiotemporal variability and drivers of CO_2 and air–sea CO_2 fluxes in the California Current System: an eddy-resolving modeling study, Biogeosciences, 11, 671–690, doi:10.5194/bg-11-671-2014, http://www.biogeosciences.net/11/671/2014/, 2014.

Walsh, J.: Importance of continental margins in the marine biogeochemical cycling of carbon and nitrogen, Nature, 350, 53–55, http://www.ccpo.odu.edu/~klinck/Reprints/PDF/walshNature91.pdf, 1991.

Wang, A. Z., Cai, W.-J., Wang, Y., and Ji, H.: The southeastern continental shelf of the United States as an atmospheric CO2 source and an exporter of inorganic carbon to the ocean, Continental Shelf Research, 25, 1917–1941, doi:10.1016/j.csr.2005.04.004, http://linkinghub.elsevier.com/retrieve/pii/S0278434305000774, 2005.

Yool, A. and Fasham, M.: An examination of the "continental shelf pump" in an open ocean general circulation model, Global Biogeochemical Cycles, 15, 831–844, http://onlinelibrary.wiley.com/doi/10.1029/2000GB001359/full, 2001.

Parameters of the biogeochemical model as in Gruber et al. (2006) Parameter Value unitsSeawater light attenuation 0.04 m^{-1}Chl-a light attenuation 0.024 $m^{-1}(mgChlam^{-3})^{-1}$Carbon to Nitrogen ratio 6.625 Ratio of $CaCO_3$ to C_{org} formation 0.07 Dissolution of $CaCO_3$ 0.0057 day^{-1}Phytoplankton Half-sat. for nitrate uptake 0.75 $mmolm^{-3}$Phytoplankton Half-sat. for ammonium uptake 0.50 $mmolm^{-3}$Phytoplankton linear mortality rate 0.024 day^{-1}max chlorophyll/carbon ratio 0.0535 $mgChla/mgC$Zoo. Grazing rate 0.6 day^{-1}Zoo. Assimilation efficiency 0.75 Grazing half-sat. for Phytoplankton 1.0 $mmolNm$Zoo. Mortality rate 0.1 $day^{-1}(mmolm^{-3})^{-1}$Zoo. Basal metab. rate 0.1 day^{-1}Zoo. Mortality alloc. fract. 0.33 Zoo. Egestion alloc. fract. 0.33 Particle coagulation rate 0.005 day^{-1}Nitrification rate 0.05 day^{-1}Nitrification inhibition threshold 0.0095 Wm^{-2}Nitrification inhibition half dose 0.036 Wm^{-2}Remin. ratio of small detritus 0.03 day^{-1}Remin. ratio of large detritus 0.01 day^{-1}Phytoplankton sinking velocity 0.5 $mday^{-1}$Small detritus sinking velocity 1.0 $mday^{-1}$Large detritus sinking velocity 10 $mday^{-1}$

Table 1. Statistic Statistical indicators of the model skill for surface ocean pCO_2 in the three areas (A1, A2 and A3 - Fig.4). The indicators are: ME (Model Efficiency); CF (Cost Function); and PB (Percentage of Bias). Additionally, showing total bias (μatm), correlation and total number of observations (N) available on each area. Bold values indicate "good/excellentor reasonable"model skillwhen comparing to the SOCAT database.

Area	ME	CF	PB	Bias	Correlation	N
A1	**0.23**	**0.52**	**2.88**	10.26	0.80	77
A2	−0.18	**0.61**	**4.23**	15.0	−0.34	60
A3	−4.70	**1.83**	**11.59**	40.4	−0.13	40

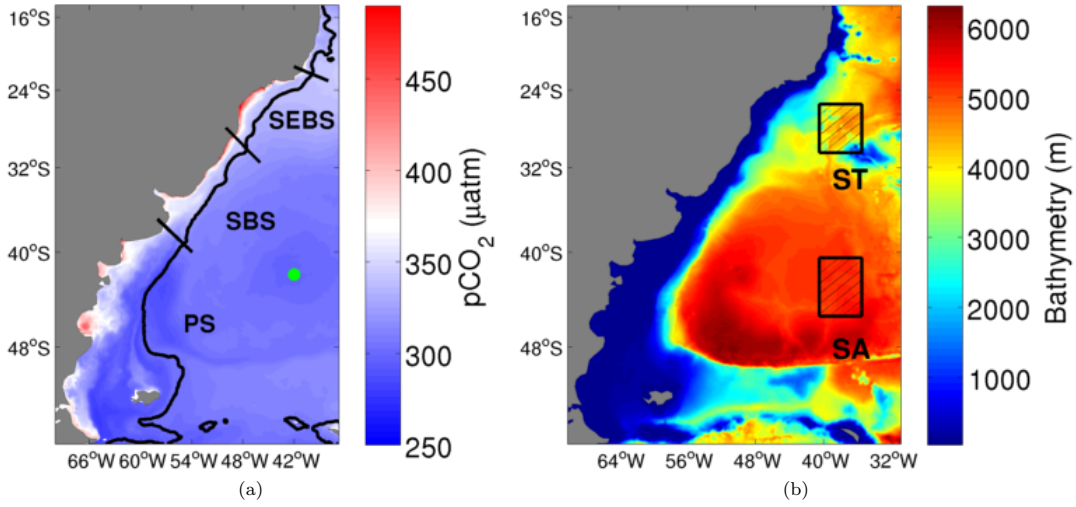

Figure 1. Areas utilised for the temporal analysis, (a) show the 3 continental shelves (SEBS, SBS and PS) analysed in a map with annual mean ocean surface pCO_2~~, the~~. The green circle represents the location of the vertical profile at the OOI site. (b) show the two oceanic regions (ST and SA) in a map with bathymetry.

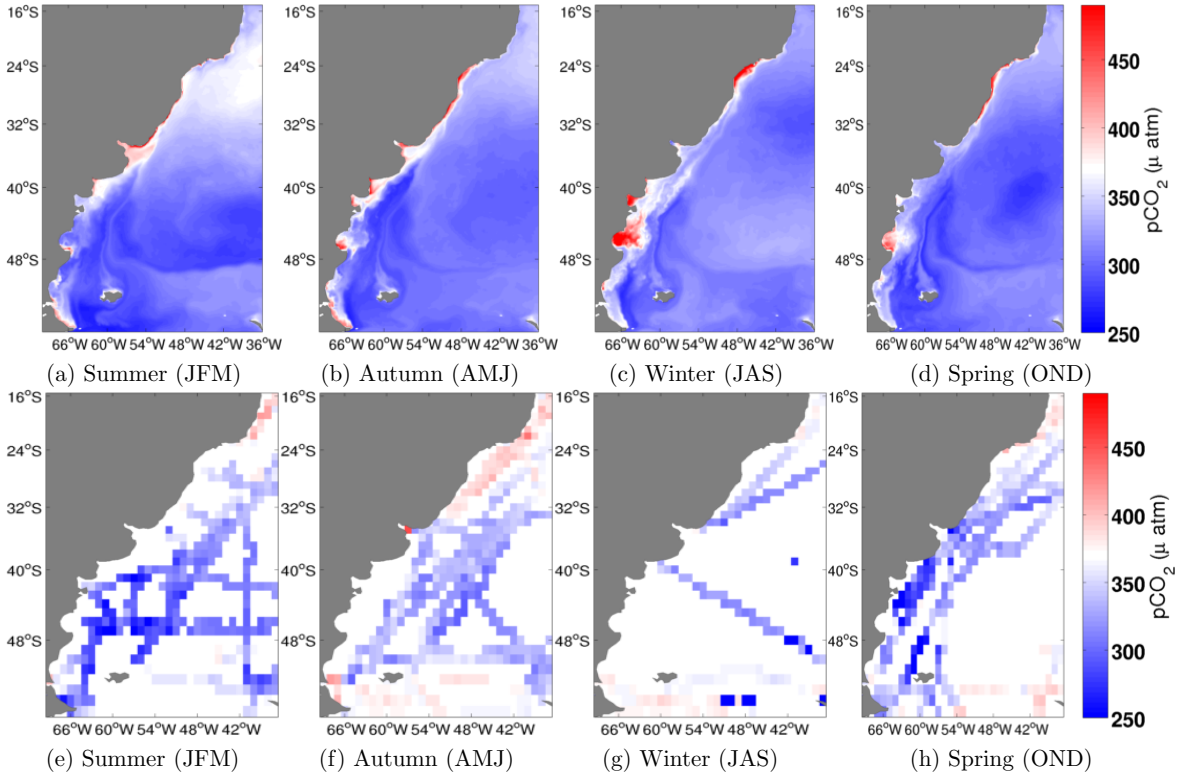

(a) Summer (JFM) (b) Autumn (AMJ) (c) Winter (JAS) (d) Spring (OND)

(e) Summer (JFM) (f) Autumn (AMJ) (g) Winter (JAS) (h) Spring (OND)

Figure 2. Seasonal climatology of modeled ~~surface~~ ocean surface pCO_2 (~~first~~ upper row) and observations of pCO_2 from the SOCAT database (~~second~~ lower row). The white separation between red and blue is set to 370 ~~μatm~~ μatm which is the atmospheric pCO_2 used in this study. Blue ~~represent~~ represents a sink of atmospheric CO_2 and red a source.

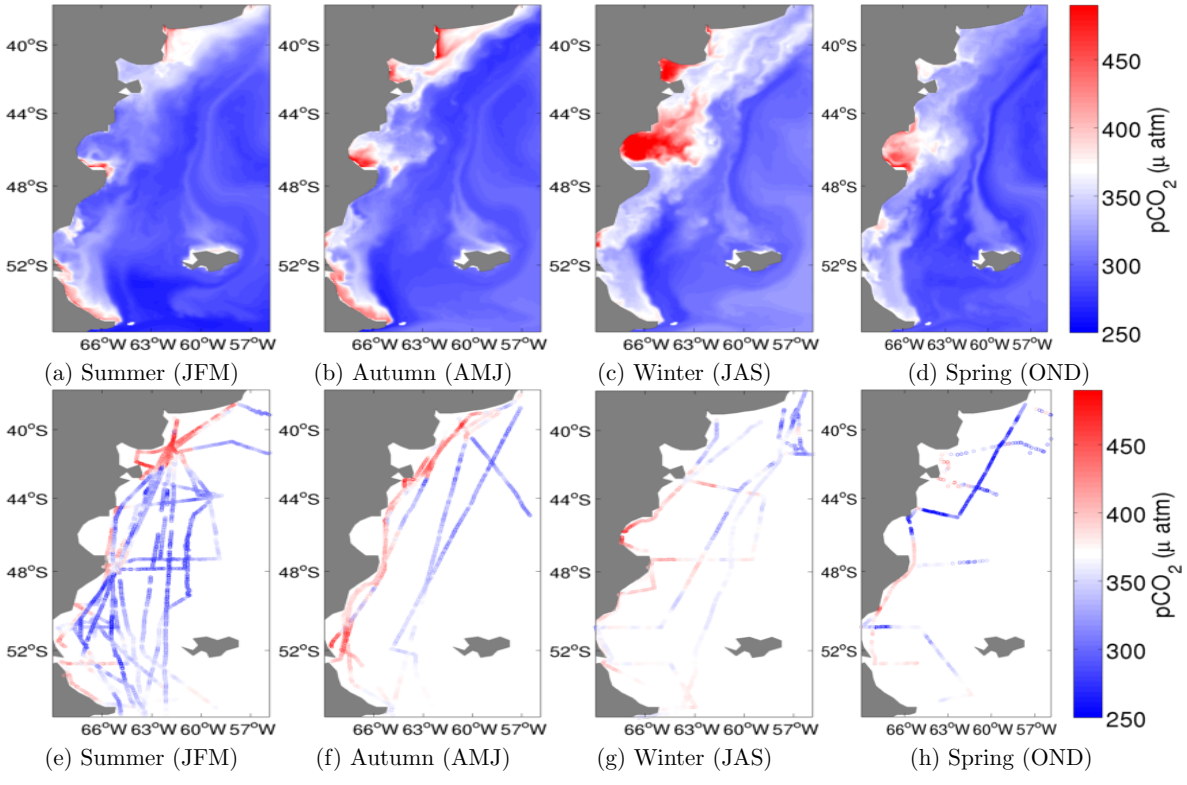

(a) Summer (JFM) (b) Autumn (AMJ) (c) Winter (JAS) (d) Spring (OND)

(e) Summer (JFM) (f) Autumn (AMJ) (g) Winter (JAS) (h) Spring (OND)

Figure 3. Model evaluation on the Patagonia Shelf (PS) (zoom in from model domain in Fig. 2a). Seasonal climatology of ~~modelled surface~~ modeled ocean surface pCO_2 (~~first~~ upper row) and pCO_2 observations from ARGAU and GEF3 cruises(~~second~~ lower row) (Bianchi et al., 2009). The white separation between red and blue is set to 370 ~~μatm~~ μatm which is the atmospheric pCO_2 used in this study. Blue ~~represent~~ represents a sink of atmospheric CO_2 and red a source.

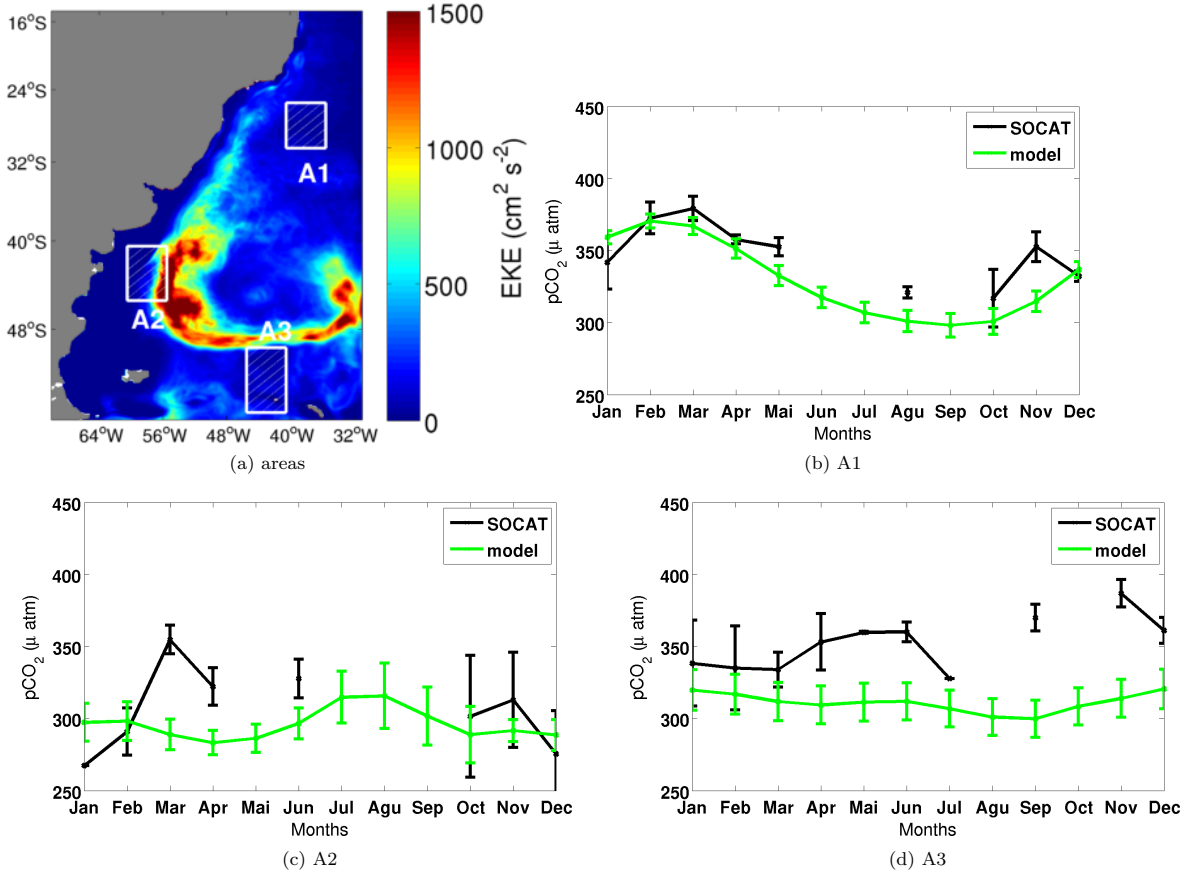

(a) areas (b) A1 (c) A2 (d) A3

Figure 4. Location of the three areas used for the monthly comparison with SOCAT database (a) in a map with annual ~~averaged~~ mean eddy kinetic energy. In figures (b), (c) and (d), green lines are the ~~modelled~~ modeled monthly mean pCO_2 and black lines are the monthly mean pCO_2 from SOCAT. Error bars are two standard deviations

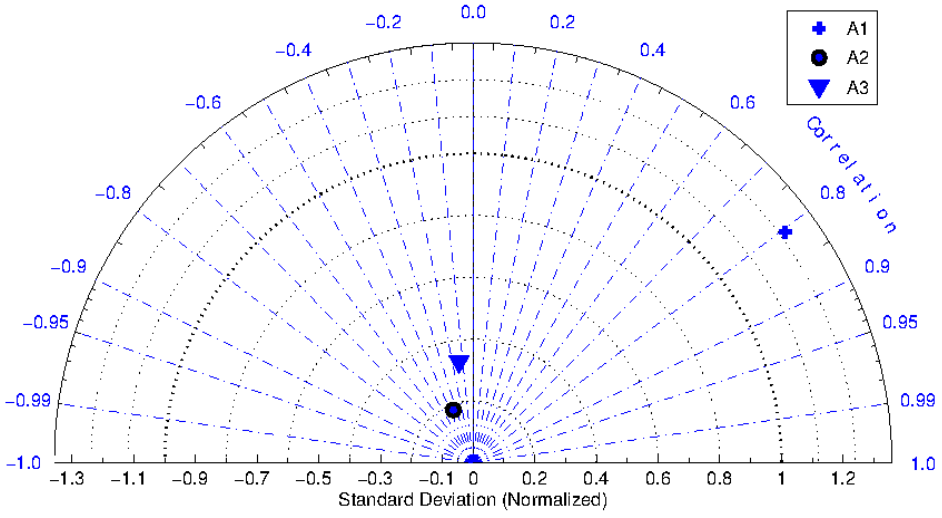

Figure 5. Taylor Diagram showing the three areas used for comparison with SOCAT observational data. A1 is the only area with statistically significant correlation.

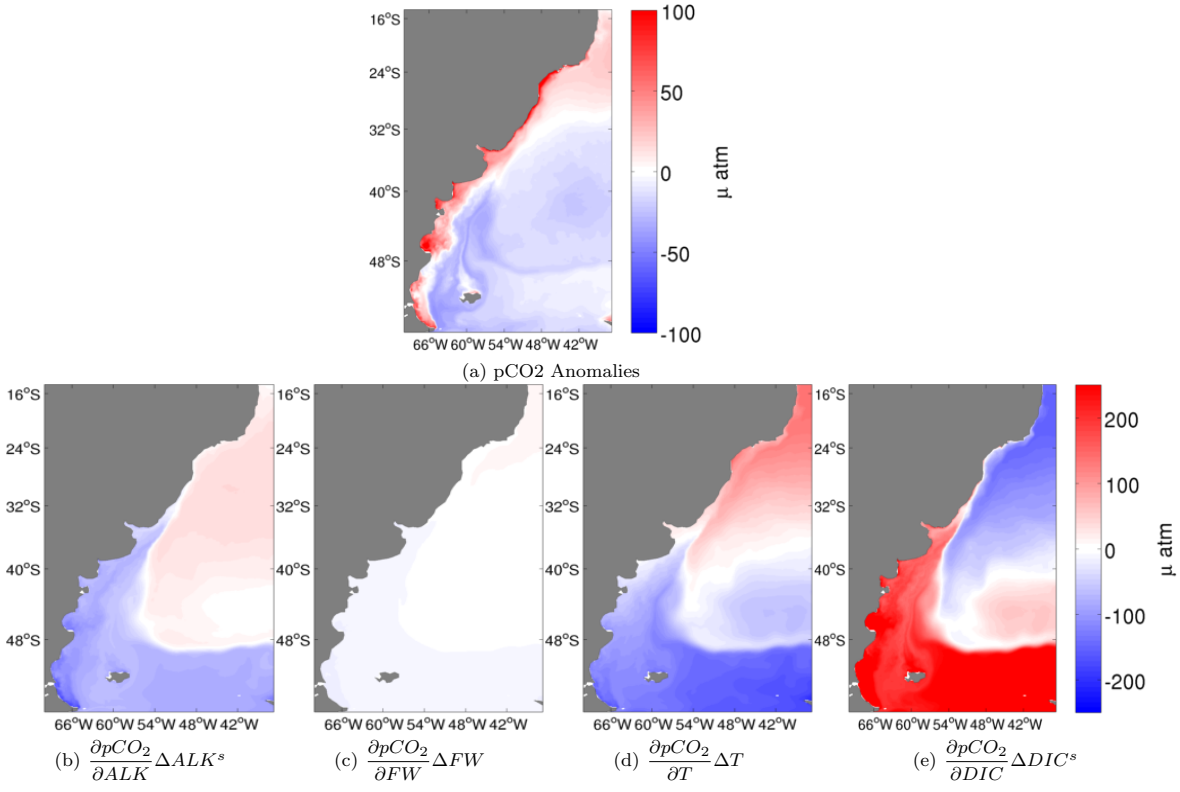

(a) pCO2 Anomalies

(b) $\frac{\partial pCO_2}{\partial ALK}\Delta ALK^s$ (c) $\frac{\partial pCO_2}{\partial FW}\Delta FW$ (d) $\frac{\partial pCO_2}{\partial T}\Delta T$ (e) $\frac{\partial pCO_2}{\partial DIC}\Delta DIC^s$

Figure 6. $p\mathrm{CO}_2$ spatial anomalies - difference between annual mean and domain mean (a) and the contribution of the main drivers: ALK^s (b), FW (c), T (d) and DIC^s (e). Computed using spatial anomalies for Δ

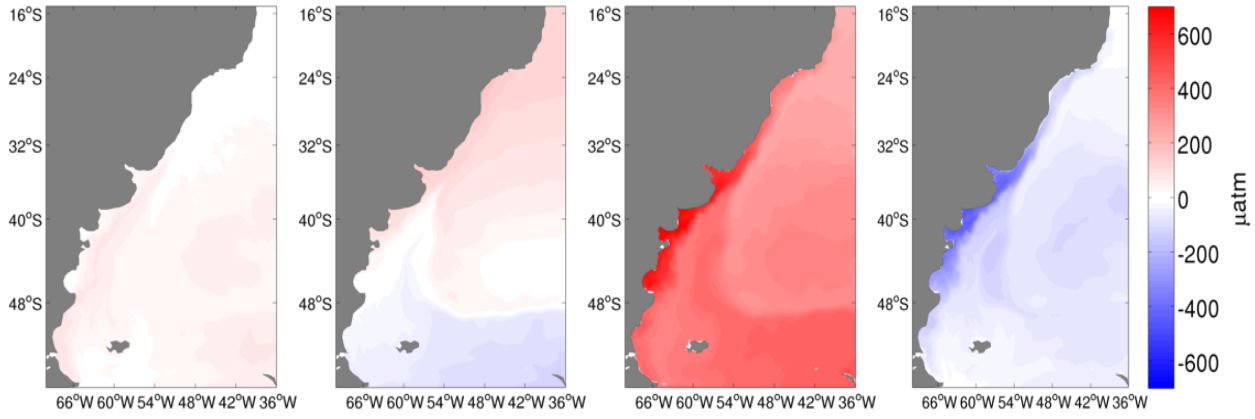

(a) Air-Sea CO_2 flux (b) CO_2 solubility (c) Physical transport (d) Biology

Figure 7. Processes driving the annual mean surface $p\mathrm{CO}_2$. Contribution of Air-sea flux of CO_2 [Control - E1] (a), CO_2 solubility [E2 - E3] (b), physical transport [E3] (c) and biological production [E1 - E2] (d)

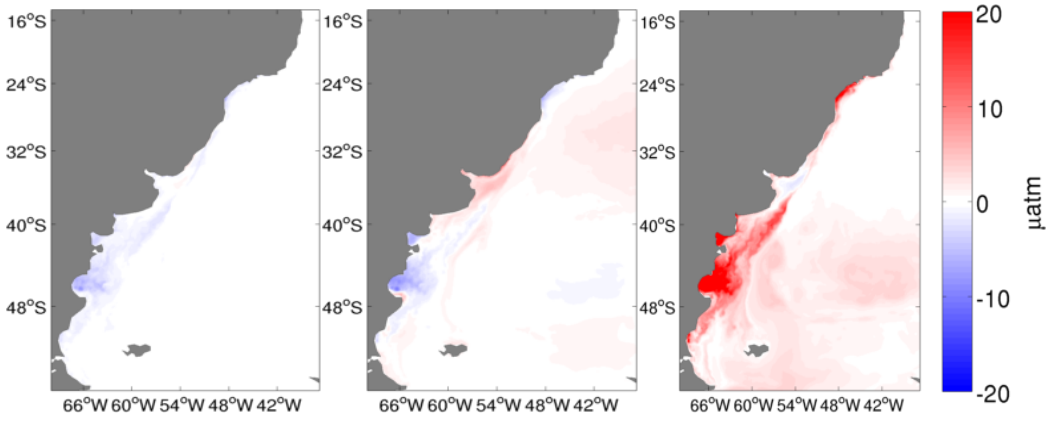

(a) $\frac{\partial pCO_2}{\partial ALK}\Delta ALK^s$ (b) $\frac{\partial pCO_2}{\partial T}\Delta T$ (c) $\frac{\partial pCO_2}{\partial DIC}\Delta DIC^s$

Figure 8. Sensitivity of $p\mathrm{CO}_2$ computed with grid point anomalies in time to local annual means. Annual ~~average~~ mean contribution of the main drivers: ALK^s (a), T (b) and DIC^s (c).

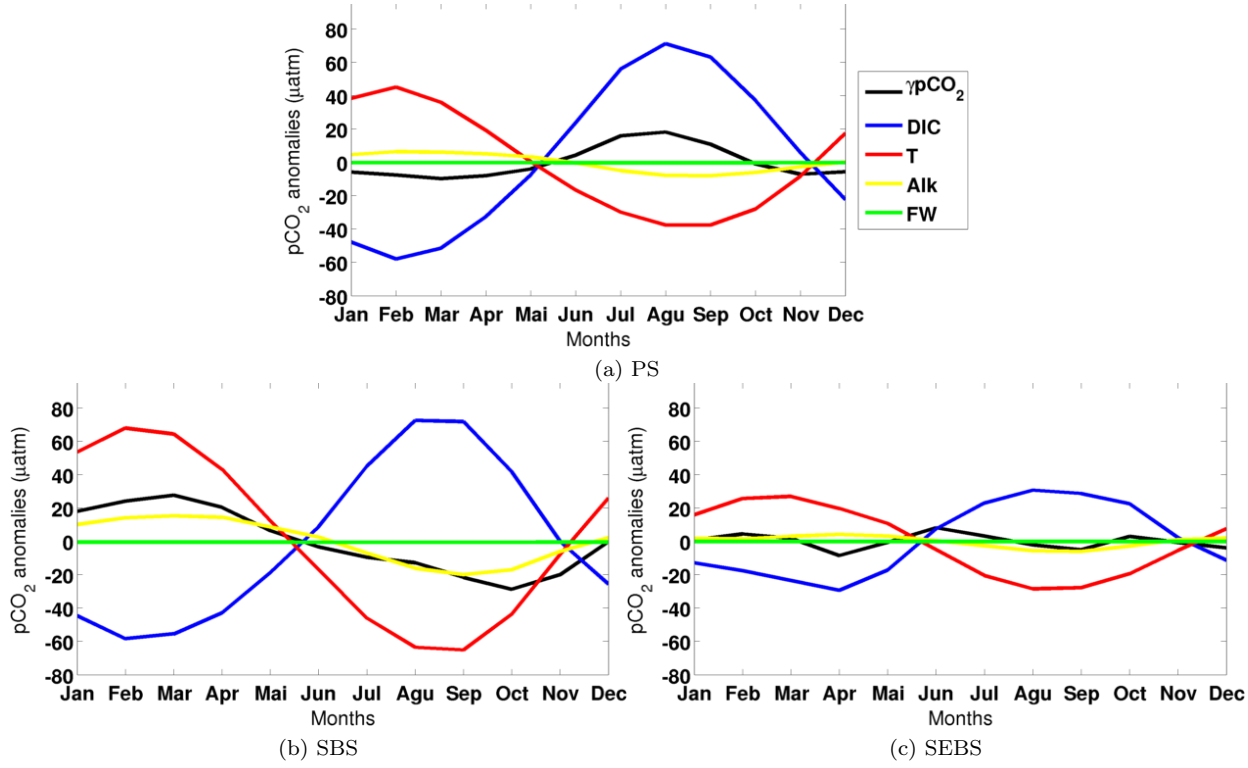

(a) PS

(b) SBS

(c) SEBS

Figure 9. Temporal evolution of $p\mathrm{CO}_2$ anomalies and their drivers in each continental shelf (right hand side of Eq. 1 using temporal anomalies), red line represents the effects of Temperature, blue line the effects of DIC^s, green line FW, and yellow line ALK^s.

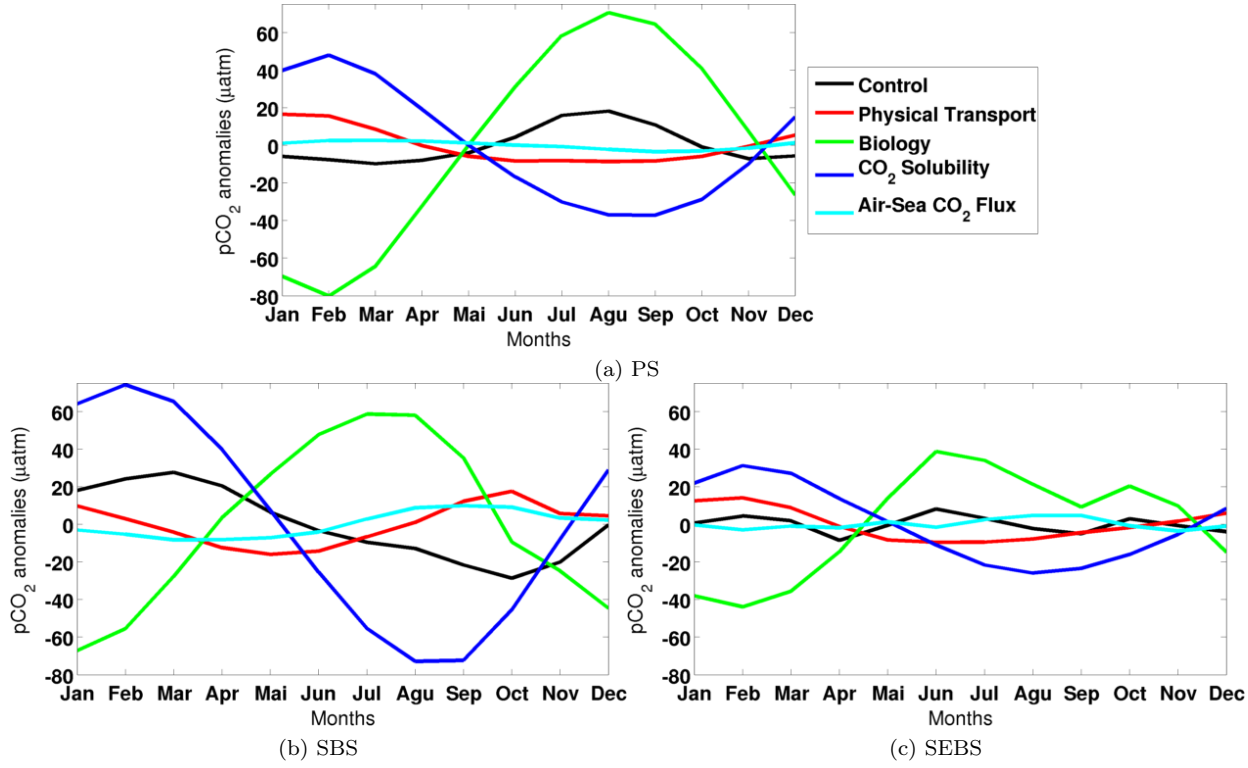

(a) PS

(b) SBS

(c) SEBS

Figure 10. temporal evolution of the monthly anomalies of each process in regulating pCO_2 anomalies, green line represents the biological production, red line the physical transport, light blue line the air-sea CO_2 fluxes and dark blue line the solubility. Black lines represent the temporal pCO_2 anomalies.

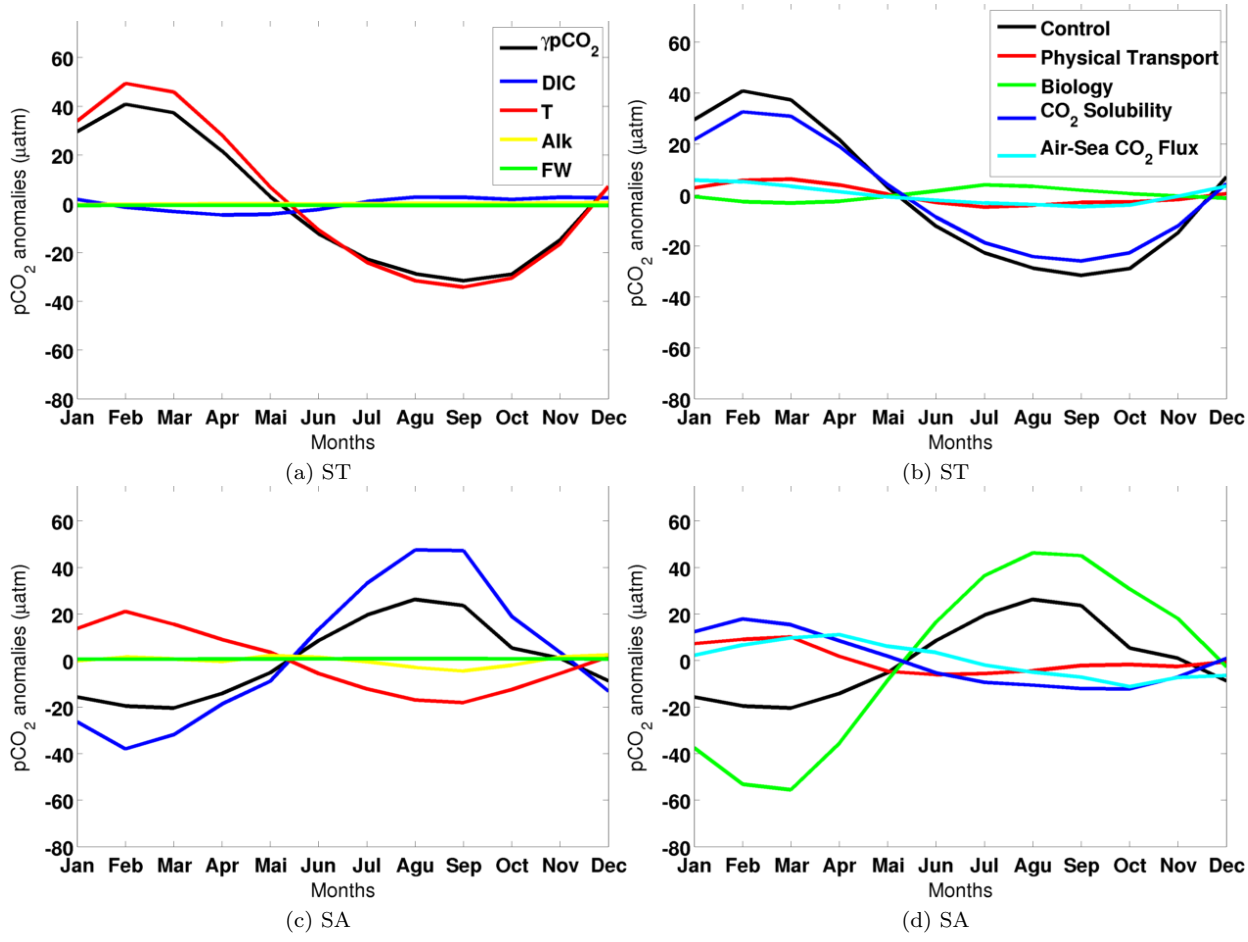

(a) ST (b) ST

(c) SA (d) SA

Figure 11. Figures (a) and (b) show the temporal evolution of $p\mathrm{CO}_2$ anomalies and its drivers in each oceanic regions (ST and SA) (right hand side of Eq. 1 using temporal anomalies), red line represents the effects of T, blue line the effects of DIC^s, green line the FW and yellow line ALK^s. Figures (c), and (e) show the temporal evolution of the monthly anomalies of each process in regulating temporal $p\mathrm{CO}_2$ anomalies, green line represents the biological production, red line the physical transport, light blue line the air-sea CO_2 fluxes and dark blue line the solubility. Black lines represent the temporal $p\mathrm{CO}_2$ anomalies.

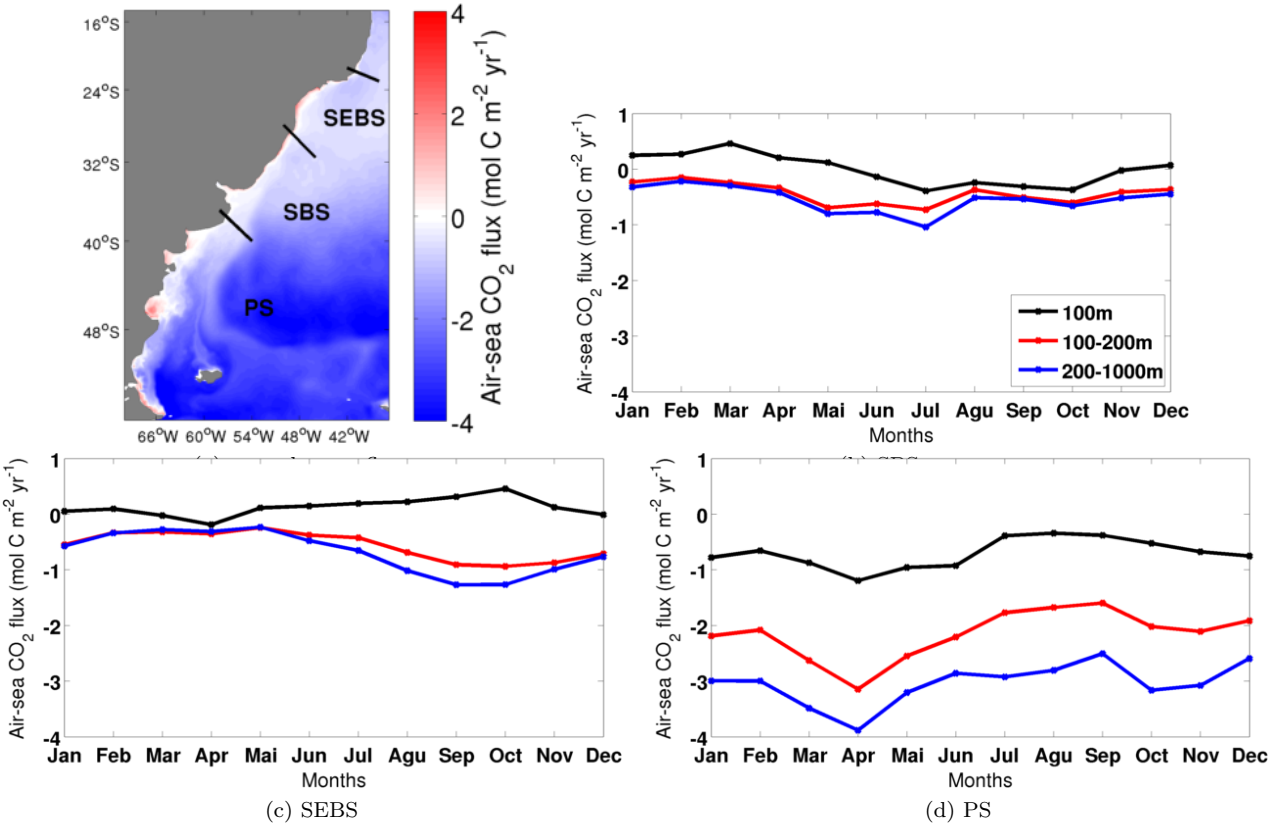

(c) SEBS (d) PS

Figure 12. Figure (a) is the annual ~~average~~ mean of air-sea CO_2 fluxes. Figures (b), (c) and (d) show the monthly average of surface CO_2 fluxes constrained to bathymetry levels of 100m, 200m and 1000m.

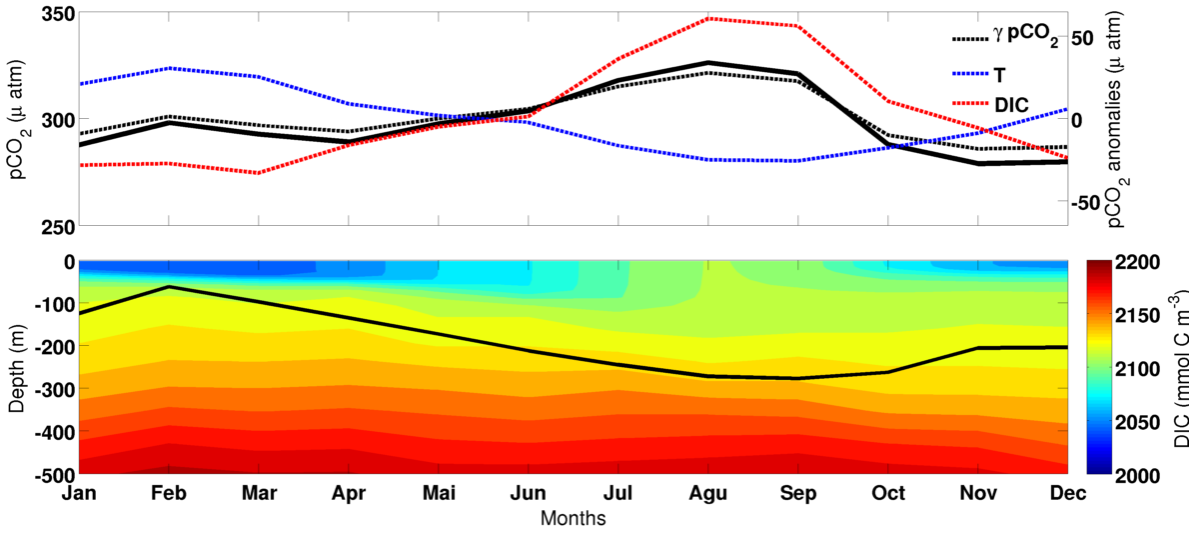

(a)

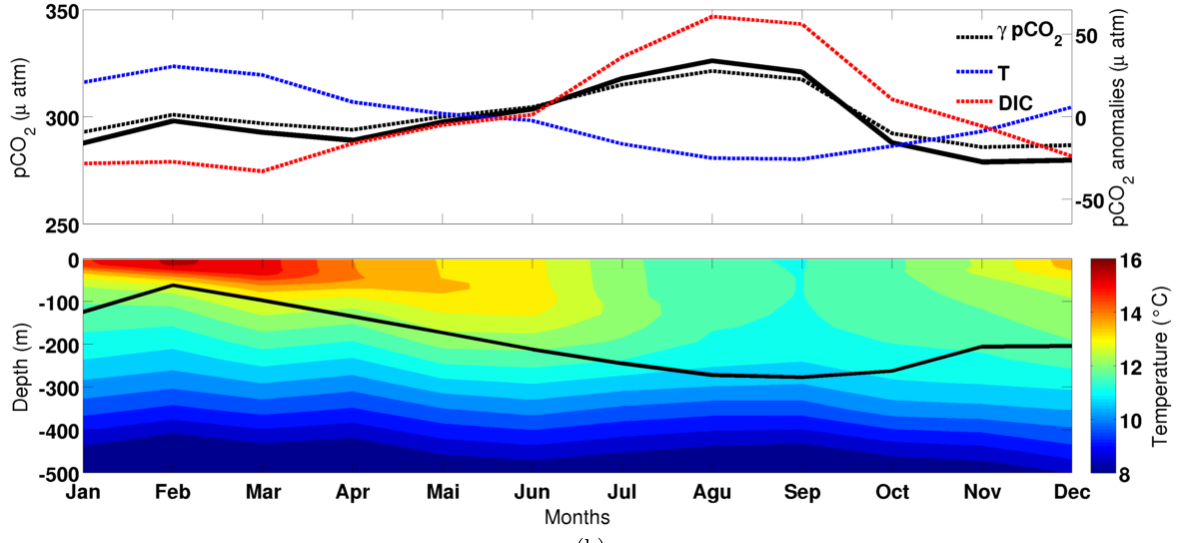

(b)

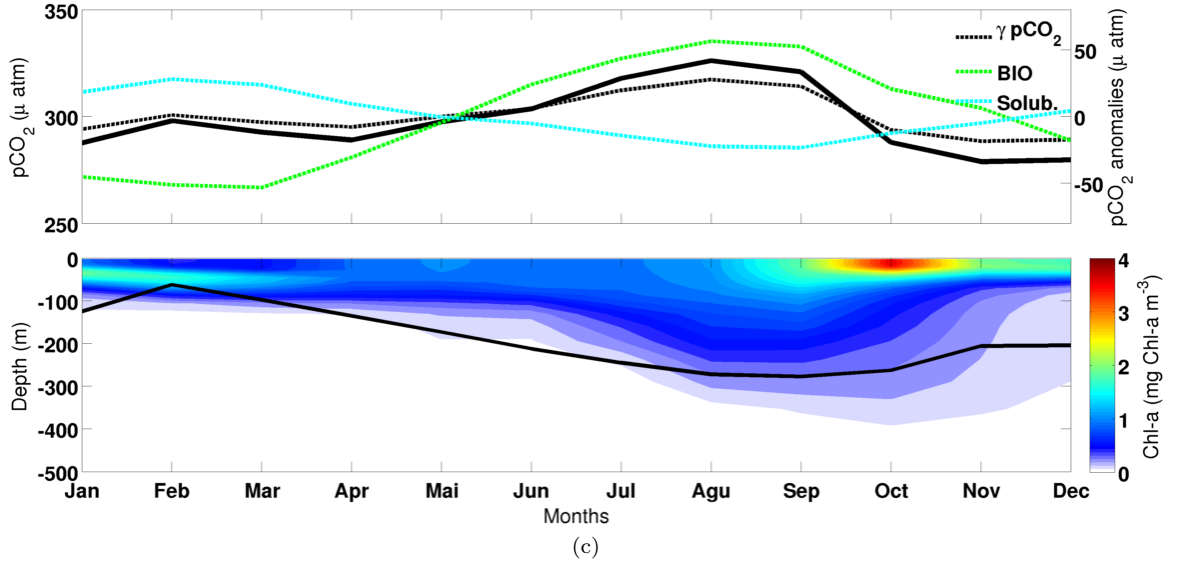

(c)

Figure 13. Vertical profile at 42°S, 42°W~~, upper~~. Upper panels showing monthly mean surface pCO_2 (solid black line), pCO_2 anomalies (dashed black line) and the contribution from ~~the main drivers (Fig. (a)~~ T and DIC^s (~~b~~red and blue dashed lines) ~~)~~ and the ~~main processes~~ contribution of biology and solubility (~~Fig. (e~~green and cyan dashed lines). Lower panels showing vertical profiles of DIC (a), T (b), and chlorophyll ~~concentration~~

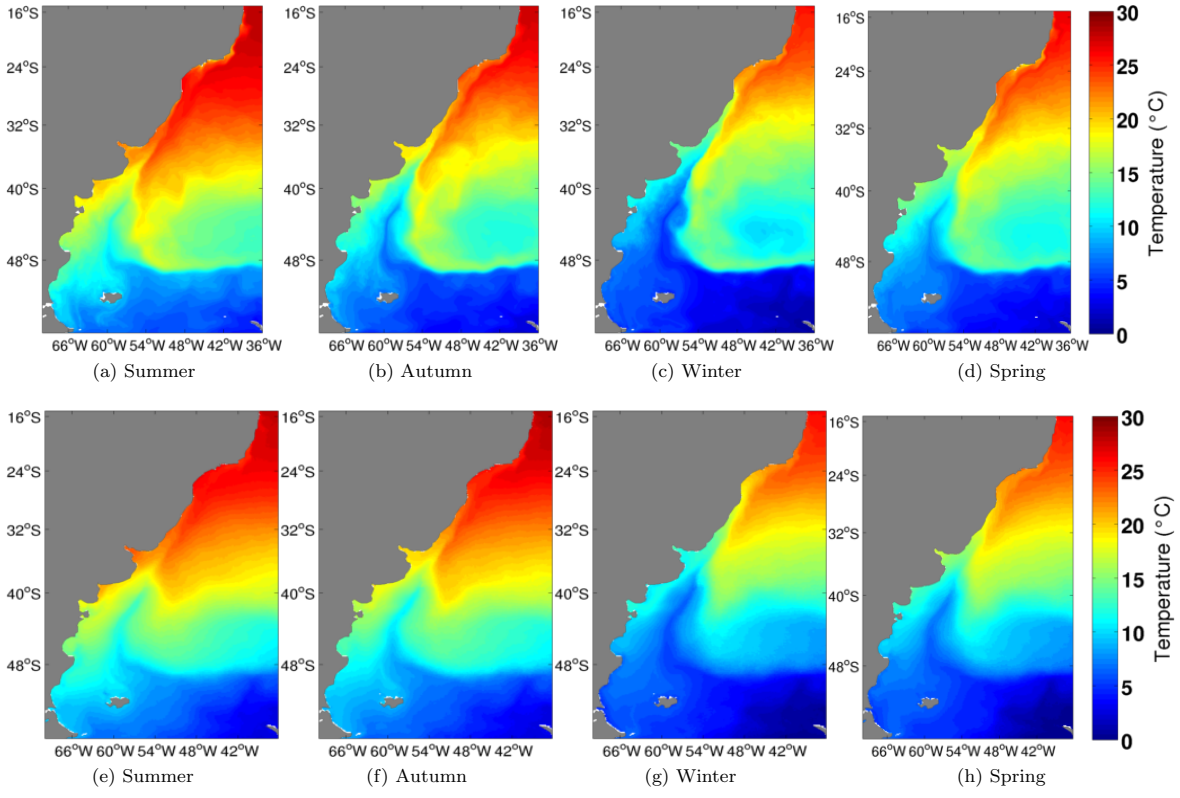

(a) Summer (b) Autumn (c) Winter (d) Spring

(e) Summer (f) Autumn (g) Winter (h) Spring

Figure 14. Seasonal climatology of modeled sea surface temperature ~~°C~~ °C - 4 years average (~~first~~ upper row), and climatology from AVHRR sensor - from 1985 to 2002 (~~second~~ lower row).

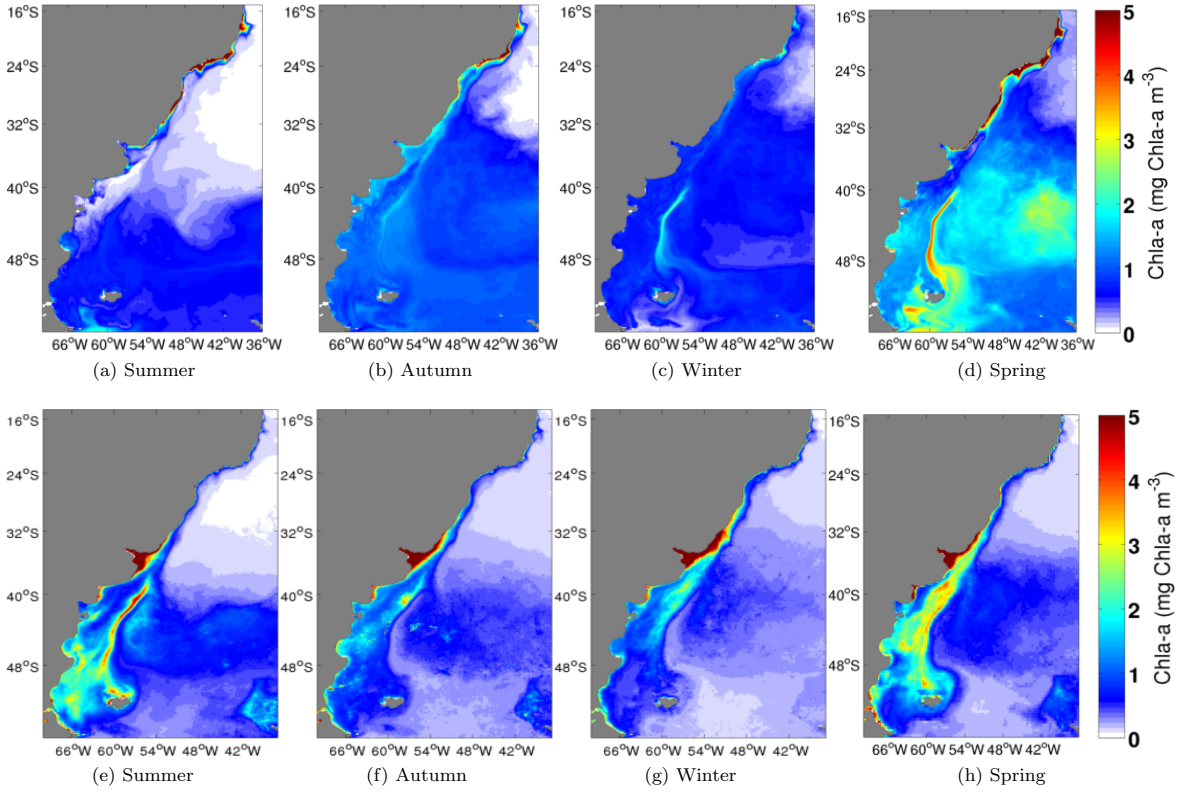

(a) Summer (b) Autumn (c) Winter (d) Spring

(e) Summer (f) Autumn (g) Winter (h) Spring

Figure 15. Seasonal climatology of modeled chlorophyll-a concentration ~~*mgChla − am*$^{-3}$~~ mgChla-a m^{-3} - 4 years average (~~first~~ upper row), and climatology from Aqua-Modis sensor - from 2003 to 2013 (~~second~~ lower row).